bioRxiv preprint doi: https://doi.org/10.1101/759886; this version posted September 8, 2019. The copyright holder for this preprint (which was not certified by peer review) is the author/funder. All rights reserved. No reuse allowed without permission.

Bacterial Hyperswarming as a Protective Response to Intestinal Stress

Weijie Chen[1, 2, *], Arpan De[1, *], Hao Li[1, *], Dana J. Lukin[3], Wendy Szymczak[4], Katherine Sun[5], Libusha Kelly[6], Justin R. Wright[7], Regina Lamendella[8], Subho Ghosh[1], Daniel B. Kearns[9], Zhen He[10, †], Christian Jobin[10], Xiaoping Luo[1, ‡], Arjun Byju[1], Shirshendu Chatterjee[11], Beng San Yeoh[12, §], Matam Vijay-Kumar[12, §], Jay X. Tang[2], Sridhar Mani[1, **]

[1]Department of Medicine, Genetics and Molecular Pharmacology, Albert Einstein College of Medicine, 1300 Morris Park Avenue, Bronx, NY 10461, USA; [2]Department of Physics, Brown University, 182 Hope Street, Providence, RI 02912, USA; [3]Jill Roberts Center for Inflammatory Bowel Disease, 1283 York Avenue, New York, NY 10065, USA; [4]Clinical Microbiology Laboratory, Montefiore Medical Center, 111 E 210th Street, Bronx, NY 10467, USA; [5]Department of Pathology, NYU Langone Health, 560 First Avenue, New York, NY 10016, USA; [6]Department of Systems & Computational Biology, and Department of Microbiology & Immunology, Albert Einstein College of Medicine, 1300 Morris Park Avenue, Bronx, NY 10461, USA; [7]Wright Labs, LLC, 419 14th Street, Huntington, PA 16652, USA; [8]Juniata College, 1700 Moore Street, Huntingdon, PA 16652, USA; [9]Department of Biology, Indiana University Bloomington, 107 S. Indiana Avenue, Bloomington, IN 47405, USA; [10]Department of Medicine, University of Florida, Gainesville, FL 32611, USA; [11]Department of Mathematics, The City College of New York, 160 Convent Avenue, New York, NY 10031, USA; [12]UT-Microbiome Consortium, Department of Physiology & Pharmacology, University of Toledo, College of Medicine & Life Sciences, 3000 Transverse Dr, Mail Stop 1008, Toledo, OH 43614, USA

* Equal contribution ** Corresponding author

† Present address: Department of Colorectal Surgery, The Sixth Affiliated Hospital of Sun Yat-Sen University, 17 Shou Gou Ling Road, Guangzhou 510655, China

‡ Present address: Institute of Chinese Materia Medica, Shanghai University of Traditional Chinese Medicine, 1200 Cailun Road, Shanghai 201203, China

§ Present address: Department of Physiology and Pharmacology, University of Toledo College of Medicine and Life Sciences, Toledo, OH 43614, USA

bioRxiv preprint doi: https://doi.org/10.1101/759886; this version posted September 8, 2019. The copyright holder for this preprint (which was not certified by peer review) is the author/funder. All rights reserved. No reuse allowed without permission.

Bacterial swarming is a conserved and distinct form of bacterial motility that allows for rapid migration over a surface. Swarming motility is often oppositely regulated and antagonistic to biofilm formation[1]. To-date, while bacterial biofilms have been associated with pathogenesis and pathobiology of human diseases (e.g., infections, inflammation and cancer)[2-4], there are very few examples of swarming behaviors that uniquely define or align with human pathophysiology (e.g., antibiotic resistance)[5,6,7]. Here we report that bacterial swarming is highly predictive of the presence of intestinal stress in mice, pigs and humans. Using a modified agar plate assay, we isolated from murine feces a novel *Enterobacter* hyperswarming strain, SM3 that demonstrated significant protection from intestinal inflammation and promoted restitution in a mouse model of colitis. As opposed to bacterial biofilms[8], we report that the swarming phenotype protects against intestinal inflammation in mice. Mechanistically, commensal swarming strains rapidly consume oxygen *in vitro* and *in vivo*, leading to a favorable anaerobic environment conducive to the growth of beneficial anaerobes. The swarming property of bacteria rather than the individual strains themselves, independently lends the ability to protect and heal from intestinal inflammation. This work identifies a new paradigm in which intestinal stress, specifically inflammation, allows for emergence of swarming bacteria, which in turn act to suppress inflammation via mechanisms that are associated in part with oxygen depletion and bloom of beneficial anaerobes.

bioRxiv preprint doi: https://doi.org/10.1101/759886; this version posted September 8, 2019. The copyright holder for this preprint (which was not certified by peer review) is the author/funder. All rights reserved. No reuse allowed without permission.

Swarming, driven by flagella, is a fundamental process in bacteria allowing for rapid movement across a surface[1,9]. This process offers bacteria a competitive advantage in occupying certain niches (e.g., seeding colonization)[10]; however, the cost-benefits to bacteria[11,12] and consequences to its host or the environment remain largely unknown[9]. There are, however, cases in which bacterial swarms lead to improved benefits for the entire bacterial community as a whole (e.g., antibiotic resistance)[13]. Here we show that bacterial swarming is a hallmark of a stressed intestine. When swarming bacteria are present in sufficient abundance, the act of swarming *per se* suppresses intestinal stress in mammals. We posit that this occurs via the creation of a conducive anaerobic environment that leads to induction of beneficial anaerobes, which are associated with mucosal healing.

To test whether bacterial swarming is associated with human and rodent gut health, we developed a modified swarming assay based on an established agar-based plate assay utilized for single species[14]. Swarming colonies are defined by existence of a clear outer surfactant layer with bacterial rim defining the swarm edge. Hyperswarming, by contrast, is defined as collective movement that allows for a plate covering morphology with or without a visible distinctive surfactant leading edge[15]. Since prototypical swarming bacteria (e.g., *Pseudomonas aeruginosa*) and its hyperswarming variants are associated with virulence[5,16], we surmised that bacterial swarming might be well represented in colonoscopy samples and feces from humans with bacterial virulence associated pathologies (e.g., intestinal inflammation)[17]. Colonoscopy aspirates were obtained from individuals with an active illness (inflammatory bowel disease - Crohn's and ulcerative colitis and other common forms of intestinal stress like intestinal polyps[18,19]) as well as age and gender matched controls (those without a clinically active illness). Within our sampling pool, bacterial hyperswarming was over-represented in cases with overt or clinically active intestinal stress (Extended Data Fig. 1a-b). We did not find a single specimen harboring

bioRxiv preprint doi: https://doi.org/10.1101/759886; this version posted September 8, 2019. The copyright holder for this preprint (which was not certified by peer review) is the author/funder. All rights reserved. No reuse allowed without permission.

hyperswarmers in our "control or non-disease" population. In this pilot evaluation, the specificity and positive predictive value of the test for disease as defined was approximately, 88 and 89%, respectively, while the sensitivity and negative predictive value of the test was only approximately 56 and 52%, respectively (Extended Data Fig. 1c). Similarly, feces collected from pigs with active inflammatory bowel disease also showed an increased prevalence of swarming bacteria as compared to control pigs (Extended Data Fig. 1d). Together, these pilot data indicate that swarming (specifically, hyperswarming) is a specific feature, and potentially a biomarker of an intestinal pathology as defined by harboring active intestinal inflammation or polyps.

To identify the relevance of swarmers on host health, we focused on isolating endogenous swarming bacteria residing in rodents and humans. On arguing the principle of selfish dominance in the Nash equilibrium (e.g., The Prisoner's Dilemma as it is applied to fate decisions in adverse times)[20,21], in our modified competitive swarming assay conditions, a mixed bacterial culture gives rise to a single bacterial species populating the leading edge of the swarm colony on agar (Extended Data Fig. 2a-b). We tested whether a singular swarming bacteria species could be detected and/or isolated from mammalian feces. Swarming assays using pooled mouse or individual human feces yielded single species of a dominant swarmer as identified by MALDI-TOF (Extended Data Table1; Extended Data Fig. 1e). To test whether swarming bacteria are also present in preclinical models, we screened feces of mice exposed to DSS, a chemical colitogen causing acute colonic inflammation[22,23]. In a single experiment, we found an identical isolate from two different mouse fecal specimens (Strains 1 and 2) – from mice exposed to water or dextran sulphate sodium (DSS), respectively (Fig. 1a). Additionally, we observed a hyperswarmer strain (Strain 3) burst from feces obtained from DSS treated mice (Fig. 1a). Hyperswarming (in feces) was uniformly absent in vehicle exposed mice (Extended Data Fig. 1e). The edge of the swarm colonies (as marked on Fig. 1a) were picked, serially passaged twice

bioRxiv preprint doi: https://doi.org/10.1101/759886; this version posted September 8, 2019. The copyright holder for this preprint (which was not certified by peer review) is the author/funder. All rights reserved. No reuse allowed without permission.

on 1% agar from a single colony and subsequently re-tested for swarm behavior on 0.5% agar plates (Fig. 1b). Interestingly, 16S rRNA gene analysis and Multi Locus Sequence Typing (Fig. 1c) identified the isolated strains to be closest to *Enterobacter asburiae*. A whole genome comparison of these *Enterobacter* strains (Fig. 1d) with related taxa *Enterobacter asburiae* and *Enterobacter cloacae*, revealed that the two strains isolated here were highly similar to each other (pairwise alignments of the strains were >99% similar over >80% of the genome), although phylogenetically distinct from the reference strains. Taken together, using an agar-based assay to isolate dominant swarmers from a heterogenous culture, we were able to isolate nearly identical strains with striking difference in their swarming potential. Strain 1 (*Enterobacter* sp. SM1) originated from feces of vehicle (water) treated mice, while strain 2 (*Enterobacter* sp. SM2) and strain 3 (*Enterobacter* sp. SM3) originated from feces of DSS-induced colitic mice. Interestingly, a quantitative PCR sequencing-based approach to specifically identify SM1 or SM3 like bacteria in feces during the evolution of DSS-induced colitis in mouse (day 0 vs day 12) showed a significant increase in its abundance, indicating increase in the population of swarmers during colitis onset (Extended Data Fig. 1f).

To determine the functional consequence of bacterial swarming in the host, DSS-induced colitic mice were administered the “near identical” swarming competent SM1 or SM3 strains. Both strains possess flagella and have the same growth rate; however, unlike SM1, SM3 is a hyperswarmer (Extended Data Fig. 3a-e; Supplementary Video 1). In contrast to that observed with SM1, SM3 significantly protected mice from intestinal inflammation (Fig. 2a-f). Specifically, SM3 significantly preserved body weight (Fig. 2a), increased colon length (Fig. 2b), reduced the colonic inflammation score (Fig. 2d), and had reduced expression of pro-inflammatory mediators compared to vehicle treated colitic mice (Fig. 2e-f). To test the mucosal healing capacity of hyperswarming bacteria, we administered strains SM1 and SM3 to mice

bioRxiv preprint doi: https://doi.org/10.1101/759886; this version posted September 8, 2019. The copyright holder for this preprint (which was not certified by peer review) is the author/funder. All rights reserved. No reuse allowed without permission.

during the recovery phase of DSS exposure[24]. SM3, as compared to SM1, significantly improved weight gain and colon length with reduced total inflammation and fibrosis at microscopic level (Extended Data Fig.4). To compare strict isogenic strains that only differed in swarming potential but not growth rate, surfactant production, or swimming speed (Extended Data Fig. 3f-j), SM3 and isogenic mutants (SM3_18 and SM3_24) (Supplementary Methods) were administered to mice exposed to DSS. SM3, but not the hyperswarming deficient mutants (SM3_18 and SM3_24), showed significant protection against weight loss, colon length and inflammation (Fig. 2g-i). Together, these data indicated that hyperswarming *per se* is necessary for anti-inflammatory activity by SM3.

To determine if the anti-inflammatory role of SM3 is dependent on the conventional intestinal microbiome composition, germ-free mice transferred to specific pathogen free conditions (GF/SPF) and exposed to DSS-induced colitis, were treated with SM3 (see methods). This strain was unable to protect against intestinal inflammation in GF/SPF mice (Fig. 3a). Fecal samples of colitic mice (conventional and GF/SPF) with SM3 administered were sent for microbiota analysis using 16S rRNA gene profiling. In contrast to GF/SPF mice, conventional mice feces showed a higher abundance of anaerobes belonging to the family S24-7 and Lactobacillaceae within SM3 treated mice when compared to vehicle mice (Fig. 3b). Specifically, in contrast with vehicle treated colitic mice, we found significant increase in the abundance of S24-7 with SM3 gavage in DSS exposed conventional mice (Fig. 3c). SM3 does not affect the microbiota of non DSS treated mice, and the levels of S24-7 bacteria remains stable in SM3 treated group compared with untreated group (Fig. 3c). Within DSS exposed conventional mice, we observed that enriched S24-7 negatively co-occur with pathogenic taxa such as the Peptostreptococcaceae and Enterobacteriaceae (Fig. 3d).

bioRxiv preprint doi: https://doi.org/10.1101/759886; this version posted September 8, 2019. The copyright holder for this preprint (which was not certified by peer review) is the author/funder. All rights reserved. No reuse allowed without permission.

The bloom of anaerobes suggests a reduction in oxygen content in the intestine. Indeed, the median concentration of oxygen in the intestinal lumen increases during inflammation[25]. Hyperswarming behavior of SM3 is observed at high concentrations of oxygen (Extended Data Fig. 5a). This motile activity in turn can consume oxygen from its immediate surroundings at a significantly higher rate than the slow swarming variants (Extended Data Fig. 5d). We hypothesized that hyperswarming activity of SM3 may also reduce luminal oxygen concentrations. We determined the oxygen concentrations within the intestinal lumen of mice at various lengths along the colon. In control conventional C57BL/6 mice, the colonic lumen is uniformly "hypoxic and/or anoxic"; however, in colitic mice, we found a significant increase in the oxygen levels (ppm) in the colonic lumen (measured at different lengths from 0.5 to 2 cm proximal to the anal verge) (Extended Data Fig. 5b). SM3 significantly reduced oxygen concentration compared to controls (vehicle); SM1 and the non-swarming mutant strains did not significantly affect oxygen concentrations compared with controls (Extended Data Fig. 5c). These results show that SM3, a hyperswarmer, but not swarming deficient strains or less dominant swarmers (i.e. SM1), consume oxygen rapidly. This activity reduces the oxygen content in the colonic lumen, where SM3 hyperswarmer is present and active, which would aid in establishing an anaerobic (micro)environment.

To generalize this concept across multiple strains, mice with DSS induced colitis were administered *B. subtilis* 3610 (wild type)[26] or its swarming deficient *swr*A isogenic mutant DS215[27] using the identical protocol as that used for SM3. In comparison with strain DS215, the wildtype significantly protects mice from intestinal inflammation (Fig. 4a-e). Similarly, swarming *Serratia marcescens* Db10, in contrast to the non-swarming JESM267 isogenic mutant, protected against inflammation in the identical mouse model (Fig. 4f-h). Incidentally, a clinical strain of *S. marcescens* (isolated from the surface washing of a human dysplastic polyp)

bioRxiv preprint doi: https://doi.org/10.1101/759886; this version posted September 8, 2019. The copyright holder for this preprint (which was not certified by peer review) is the author/funder. All rights reserved. No reuse allowed without permission.

also protected against DSS induced inflammation in mice (Supplementary Discussion). Similar to SM3, the swarming strains of *Bacillus* and *Serratia* consume oxygen significantly faster than the isogenic non-swarming strains (Extended data Fig. 5e-f). These data suggest that a common mechanism might exist among swarmers, in that, via depletion of local oxygen concentrations they all induce a favorable anaerobic environment. In addition, considering that the intestinal mucosa is relatively uneven during inflammation due to loss of mucin[28], we conjectured that swarmers or hyperswarmers may have an added advantage in niche dominance on inflamed tissue. Indeed, a mucosal race assay (Supplementary Discussion) showed that a swarming bacteria finds advantage in motility on a colitic mucosa compared to normal mucosa (Extended Data Fig. 6, Supplementary Video 2-4).

Together these studies demonstrate that intestinal inflammation promotes a niche conducive for bacterial swarming. The inflammatory milieu provides a permissive environment for stress adaptation and swarming behavior. Provided sufficient colonies form during inflammation, swarming strains deplete luminal oxygen content and allow for the intestine to re-establish conditions conducive to the growth of beneficial anaerobes. Consequently, swarming behavior could in turn suppress host inflammation by re-establishing homeostatic anaerobiosis in the gut (Extended Data Fig. 7). Furthermore, our studies demonstrate the potential for a new personalized “probiotic” approach stemming from the ability to isolate and bank swarming microbes during colitis flares. These could be stored and provided back to the same individuals to prevent colitic episodes or as a therapeutic during acute colitis. In summary, our work demonstrates the unique and unprecedented role that bacterial swarming plays in intestinal homeostasis and in the potential clinical treatment of inflammatory bowel diseases.

bioRxiv preprint doi: https://doi.org/10.1101/759886; this version posted September 8, 2019. The copyright holder for this preprint (which was not certified by peer review) is the author/funder. All rights reserved. No reuse allowed without permission.

Figure 1

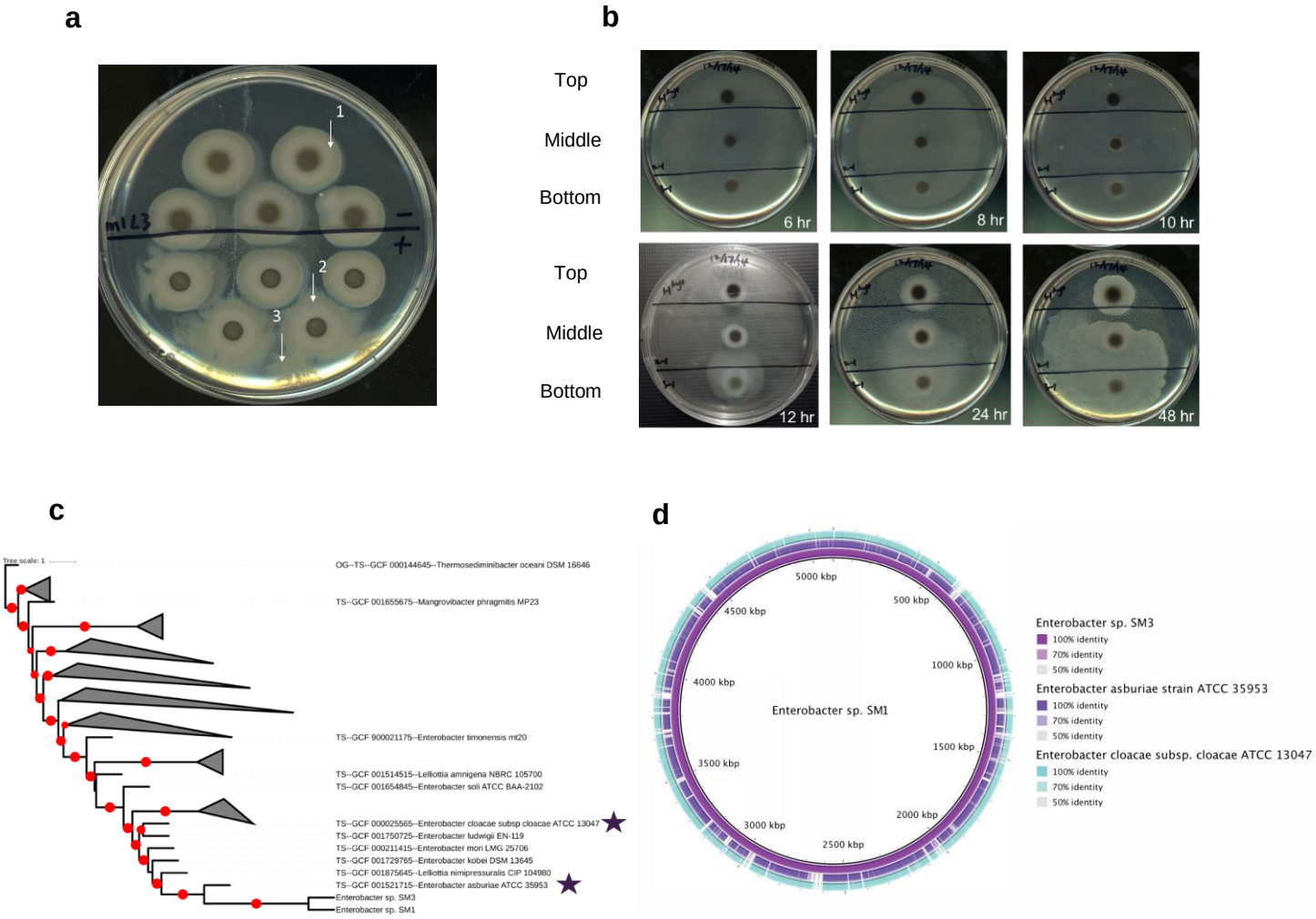

Figure 1 | Isolation and characterization of *Enterobacter* sp. a, Five replicate fecal spots from pooled fecal pellets of mice administered water (above black line) or 3% DSS water (below black line) (n = 3, day 7). The white arrows indicate 1, swarm edge isolation from control feces (SM1); 2, swarm edge isolation from feces of mice exposed to DSS (SM2); 3, swarm colony isolation from spontaneous "burst" activity from feces at 24h from plating (SM3).The mouse experiments were repeated at least twice. **b,** The bacterial clones isolated from **a** were re-plated as pure strains on 0.5% LB agar and the swarming assay performed over time. Two solid black marker lines divide each plate into 3 regions, holding spots of the 3 strains – Top: Strain 1 (SM1), Middle: Strain 2 (SM2), Bottom: Strain 3 (SM3). These strains have been repeatedly (≥ 25 times) plated in swarming assays from all aliquots stored from the original isolation (August 2014) and the results confirm that SM3 is a stable hyperswarmer. **c**, Phylogenetic tree showing multi-locus sequencing typing-based genetic relatedness between Enterobacter sp. SM1, SM3 and reference genomes. Tree was generated with autoMLST (CITE) and drawn using iTOL (CITE). Red dots indicate bootstrap support > 0.8. Stars represent related strains used for comparison with the genome sequences of SM1 and SM3 in panel **d**. **d,** Genome comparison of related *Enterobacter* strains. *Enterobacter* sp. SM1 was compared to *Enterobacter* sp. SM3 (purple) and the related strains *Enterobacter asburiae* ATCC 35953 (violet) and *Enterobacter cloacae* ATCC 13047 (cyan), and plotted in BLAST Ring Generator (BRIG) http://brig.sourceforge.net/ PMID: 21824423. DSS, Dextran Sulfate Sodium; LB, Luria-Bertani broth.

bioRxiv preprint doi: https://doi.org/10.1101/759886; this version posted September 8, 2019. The copyright holder for this preprint (which was not certified by peer review) is the author/funder. All rights reserved. No reuse allowed without permission.

Figure 2

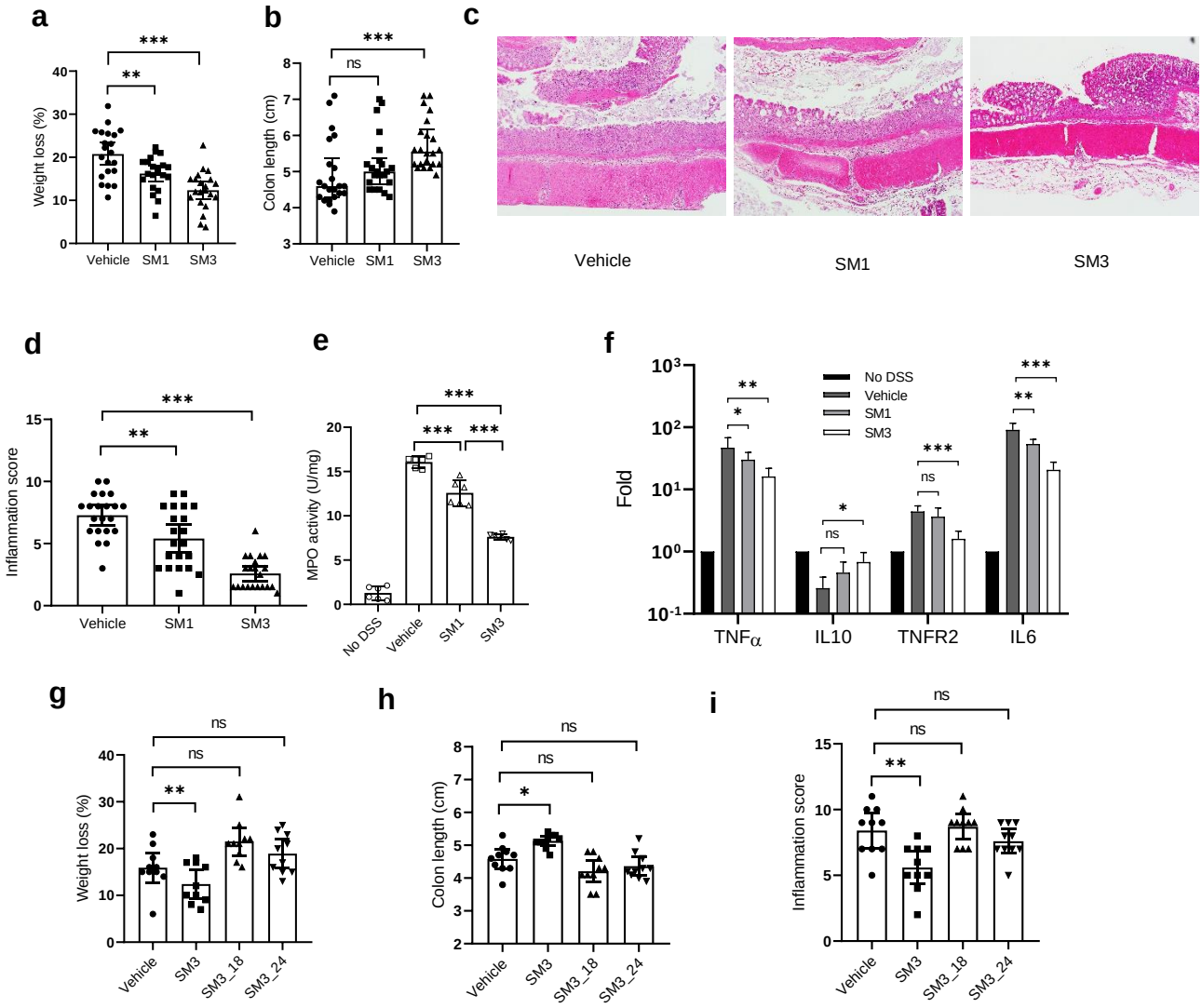

Figure 2 | Effects of *Enterobacter* sp. SM strains on DSS induced colitis in C57BL/6 mice. a-f, 8-week old mice were exposed to DSS water and treated with vehicle (LB), SM1 or SM3 by oral gavage for 10 days. **a-b** indicates weight loss (**a**) and colon length (**b**) (n = 21 per treatment group). **c**, Representative images (100x magnification) of H&E stained colonic section treated with vehicle (left), SM1 (middle) and SM3 (right). **d,** Inflammation score (n = 21 per treatment group). **e-f,** In a separate experiment, myeloperoxidase (MPO) enzyme activity was determined (n= 3, each in duplicate) (**e**). Colon total RNA (n = 4) was isolated and reverse transcribed to cDNA. RT-qPCR data show fold induction of mRNA (TNFα, IL10, TNFR2, IL6). PCR was repeated in quadruplicate. The expression was normalized to internal control, TBP. The entire experiment was repeated n = 2 for reproducibility (**f**). **g-i,** In a separate experiment, C57BL/6 mice (8-week old) were exposed to DSS water and administered vehicle (LB), SM3, or its mutants (SM3_18 or SM3_24) for 10 days. **g-i** indicates weight loss (**g**), colon length (**h**) and inflammation score (**i**) (n = 10 per treatment group). Unless otherwise noted, data are represented as mean and 95% CI, and significance tested using one-way ANOVA followed by Tukey's post hoc test. **c,** data represented as median and interquartile range, and significance tested using Kruskal-Wallis followed by Dunn's multiple comparisons test. * $P < 0.05$; ** $P < 0.01$; *** $P < 0.001$; ns, not significant. H&E, Hematoxylin and Eosin; TBP, TATA-Box Binding Protein; CI, Confidence Interval.

bioRxiv preprint doi: https://doi.org/10.1101/759886; this version posted September 8, 2019. The copyright holder for this preprint (which was not certified by peer review) is the author/funder. All rights reserved. No reuse allowed without permission.

Figure 3

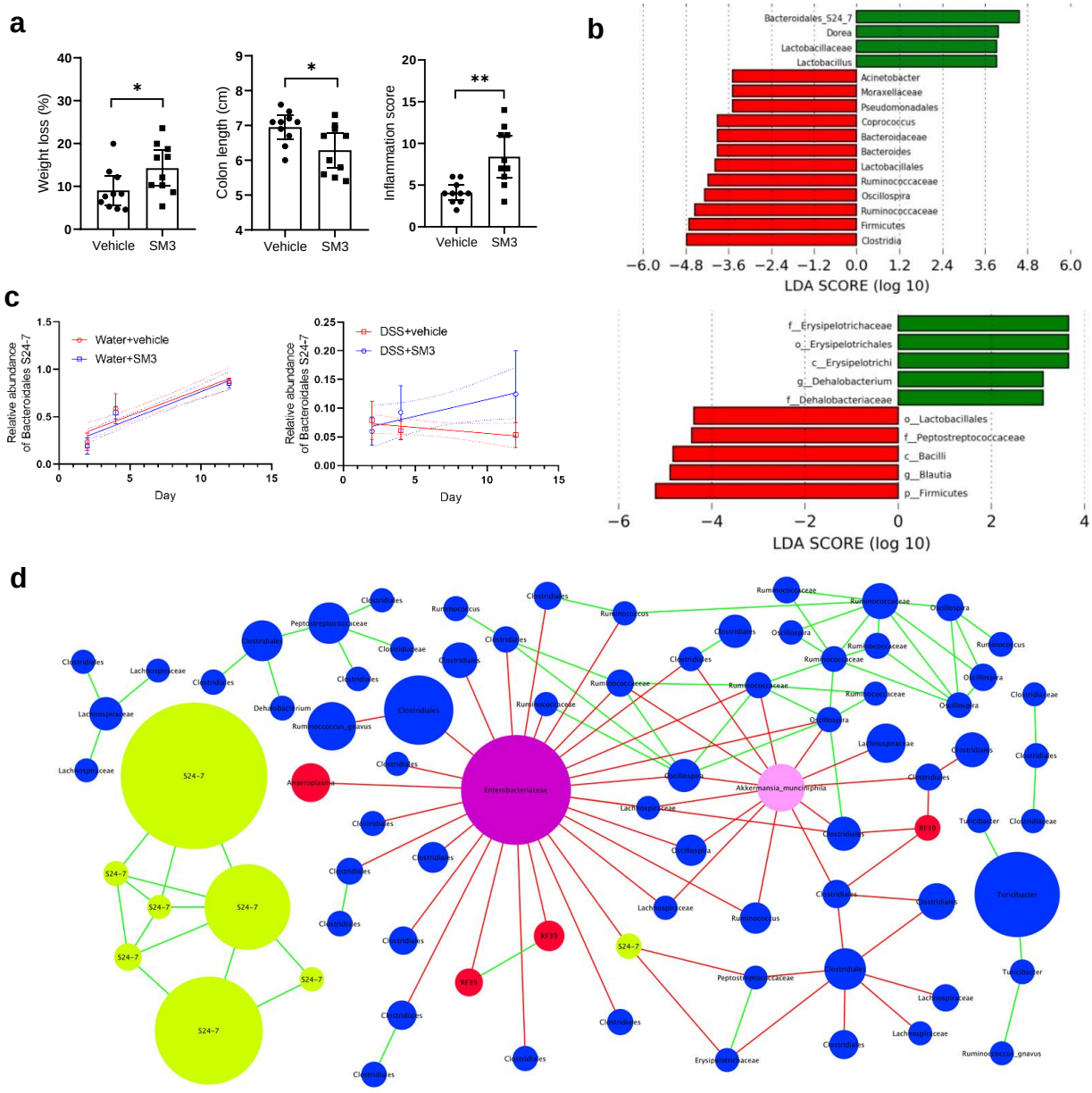

Figure 3 | Effects of SM3 on the intestinal microbiota of GF/SPF and conventional mice. a, C57BL/6 GF/SPF mice (5-week old) were exposed to DSS water and treated with vehicle (LB) or SM3 for 6 days. **a** indicates weight loss (left), colon length (middle), and inflammation score (right) (n = 10 per treatment group). **b,** Linear discriminant analysis (LDA) Effect Size (LEfSe) plot of taxonomic biomarkers identified using feces of SM3 treated conventional (n = 10) (upper) and GF/SPF (n = 10) (lower) colitic mice on day 12 and day 6, respectively, as compared to vehicle (n = 10). Green and red bars indicate bacterial enrichment within SM3 treated and vehicle group respectively. All taxa that yielded an LDA score >3.0 are presented. **c,** Relative abundance of S24-7 in the feces from DSS (right) and control (left) mice treated with SM3 or vehicle (n = 8 per treatment group). Linear regression line was fit to show the trend of the change (dotted lines show the 95% confidence bands). The slope of the SM3 treated group is similar to vehicle in water control group (P = 0.7827), but significantly different in DSS group (P = 0.0182). **d,** Co-occurrence network plot showing strong positive and negative correlations (Spearman's $|\rho| > 0.7$) between OTU abundances. Each node represents a single OTU and the size of each node is proportional to the relative abundance of each OTU. Green lines connecting two nodes indicate a strong positive correlation (spearman's $\rho > 0.7$) between the taxa, whereas red lines indicate a strong negative correlation (spearman's $\rho < -0.7$) between the taxa. Unless otherwise noted, data are represented as mean and 95% CI, and significance tested using a two-tailed Student's t-test. OTU, Operational Taxonomic Unit; GF/SPF, Germ-Free mice transferred to specific pathogen free conditions.

bioRxiv preprint doi: https://doi.org/10.1101/759886; this version posted September 8, 2019. The copyright holder for this preprint (which was not certified by peer review) is the author/funder. All rights reserved. No reuse allowed without permission.

Figure 4

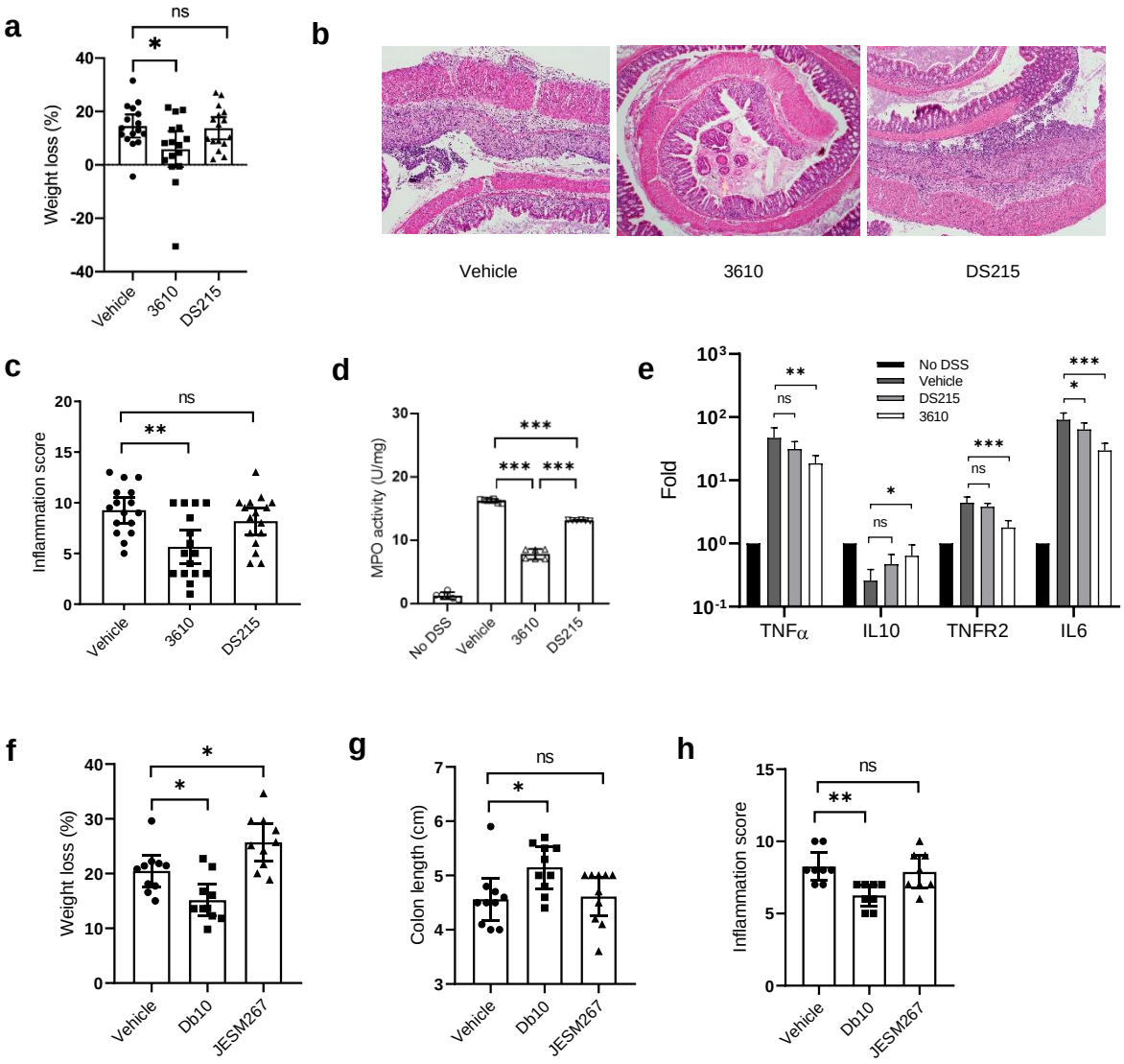

Figure 4 | Effects of *B. subtilis* and *S. marcescens* on DSS induced colitis in C57BL/6 mice. a-e, 8-week old mice were exposed to DSS water and treated with vehicle (LB), *B. subtilis* 3610 or *B. subtilis* DS215 by oral gavage for 10 days. **a,** Weight loss (n =16 per treatment group). **b,** Representative images (100x magnification) of H&E stained colonic section treated with vehicle (left), 3610 (middle) and DS215 (right). **c,** Inflammation score (n =16 per treatment group). **d-e,** In a separate experiment, myeloperoxidase (MPO) enzyme activity was determined (n= 3, each in duplicate) (**d**). Colon total RNA (n = 4) were isolated and reverse transcribed to cDNA. RT-qPCR data show fold induction of mRNA (TNFα, IL10, TNFR2, IL6). PCR was repeated in quadruplicate. The expression was normalized to internal control, TBP. The entire experiment was repeated n = 2 for reproducibility (**e**). **f-h,** In a separate experiment, C57BL/6 mice (8-week old) were exposed to DSS water and administered vehicle (LB), *S. marcescens* Db10 or *S. marcescens* JESM267 for 10 days. **f-h** indicates weight loss (**f**), colon length (**g**) and inflammation score (**h**) (n = 10 per treatment group except for **h**, for which n = 8; two colon specimens per group were used for other experiments). Unless otherwise noted, data represented as mean and 95% CI, and significance tested using one-way ANOVA followed by Tukey's post hoc test. **g,** data represented as median and interquartile range, and significance tested using Kruskal-Wallis followed by Dunn's multiple comparisons test.

bioRxiv preprint doi: https://doi.org/10.1101/759886; this version posted September 8, 2019. The copyright holder for this preprint (which was not certified by peer review) is the author/funder. All rights reserved. No reuse allowed without permission.

References

1 Verstraeten, N. *et al.* Living on a surface: swarming and biofilm formation. *Trends in microbiology* **16**, 496-506, doi:10.1016/j.tim.2008.07.004 (2008).

2 Dejea, C. M. *et al.* Microbiota organization is a distinct feature of proximal colorectal cancers. *Proceedings of the National Academy of Sciences of the United States of America* **111**, 18321-18326, doi:10.1073/pnas.1406199111 (2014).

3 Villanueva, M. T. Metabolism: Bacterial biofilms may feed colon cancer. *Nature reviews. Cancer* **15**, 320, doi:10.1038/nrc3970 (2015).

4 Johnson, C. H. *et al.* Metabolism links bacterial biofilms and colon carcinogenesis. *Cell metabolism* **21**, 891-897, doi:10.1016/j.cmet.2015.04.011 (2015).

5 Breidenstein, E. B., de la Fuente-Nunez, C. & Hancock, R. E. Pseudomonas aeruginosa: all roads lead to resistance. *Trends in microbiology* **19**, 419-426, doi:10.1016/j.tim.2011.04.005 (2011).

6 Butler, M. T., Wang, Q. & Harshey, R. M. Cell density and mobility protect swarming bacteria against antibiotics. *Proceedings of the National Academy of Sciences of the United States of America* **107**, 3776-3781, doi:10.1073/pnas.0910934107 (2010).

7 Rozalski, A., Sidorczyk, Z. & Kotelko, K. Potential virulence factors of Proteus bacilli. *Microbiology and molecular biology reviews : MMBR* **61**, 65-89 (1997).

8 von Rosenvinge, E. C., O'May, G. A., Macfarlane, S., Macfarlane, G. T. & Shirtliff, M. E. Microbial biofilms and gastrointestinal diseases. *Pathogens and disease* **67**, 25-38, doi:10.1111/2049-632x.12020 (2013).

9 Kearns, D. B. A field guide to bacterial swarming motility. *Nature reviews. Microbiology* **8**, 634-644, doi:10.1038/nrmicro2405 (2010).

10 Barak, J. D., Gorski, L., Liang, A. S. & Narm, K. E. Previously uncharacterized Salmonella enterica genes required for swarming play a role in seedling colonization. *Microbiology (Reading, England)* **155**, 3701-3709, doi:10.1099/mic.0.032029-0 (2009).

11 Butler, M. T., Wang, Q. & Harshey, R. M. Cell density and mobility protect swarming bacteria against antibiotics. *Proceedings of the National Academy of Sciences of the United States of America* **107**, 3776-3781, doi:10.1073/pnas.0910934107 (2010).

12 Finkelshtein, A., Roth, D., Ben Jacob, E. & Ingham, C. J. Bacterial Swarms Recruit Cargo Bacteria To Pave the Way in Toxic Environments. *mBio* **6**, doi:10.1128/mBio.00074-15 (2015).

13 Meredith, H. R., Srimani, J. K., Lee, A. J., Lopatkin, A. J. & You, L. Collective antibiotic tolerance: mechanisms, dynamics and intervention. *Nature chemical biology* **11**, 182-188, doi:10.1038/nchembio.1754 (2015).

14 Morales-Soto, N. *et al.* Preparation, imaging, and quantification of bacterial surface motility assays. *Journal of visualized experiments : JoVE*, doi:10.3791/52338 (2015).

15 van Ditmarsch, D. *et al.* Convergent evolution of hyperswarming leads to impaired biofilm formation in pathogenic bacteria. *Cell reports* **4**, 697-708, doi:10.1016/j.celrep.2013.07.026 (2013).

bioRxiv preprint doi: https://doi.org/10.1101/759886; this version posted September 8, 2019. The copyright holder for this preprint (which was not certified by peer review) is the author/funder. All rights reserved. No reuse allowed without permission.

16 Overhage, J., Bains, M., Brazas, M. D. & Hancock, R. E. Swarming of Pseudomonas aeruginosa is a complex adaptation leading to increased production of virulence factors and antibiotic resistance. *Journal of bacteriology* **190**, 2671-2679, doi:10.1128/jb.01659-07 (2008).

17 Yang, Y. & Jobin, C. Microbial imbalance and intestinal pathologies: connections and contributions. *Disease models & mechanisms* **7**, 1131-1142, doi:10.1242/dmm.016428 (2014).

18 Jass, J. R. Hyperplastic-like polyps as precursors of microsatellite-unstable colorectal cancer. *Am J Clin Pathol.* **119**, 773-775 (2003).

19 Crespo-Sanjuán, J. *et al.* Early detection of high oxidative activity in patients with adenomatous intestinal polyps and colorectal adenocarcinoma: myeloperoxidase and oxidized low-density lipoprotein in serum as new markers of oxidative stress in colorectal cancer. *Lab Med.* **46**, 123-135 (2015).

20 Lambert, G., Vyawahare, S. & Austin, R. H. Bacteria and game theory: the rise and fall of cooperation in spatially heterogeneous environments. *Interface focus* **4**, 20140029, doi:10.1098/rsfs.2014.0029 (2014).

21 Schultz, D., Wolynes, P. G., Ben Jacob, E. & Onuchic, J. N. Deciding fate in adverse times: sporulation and competence in Bacillus subtilis. *Proceedings of the National Academy of Sciences of the United States of America* **106**, 21027-21034, doi:10.1073/pnas.0912185106 (2009).

22 Perse, M. & Cerar, A. Dextran sodium sulphate colitis mouse model: traps and tricks. *Journal of biomedicine & biotechnology* **2012**, 718617, doi:10.1155/2012/718617 (2012).

23 Chassaing, B., Aitken, J. D., Malleshappa, M. & Vijay-Kumar, M. Dextran sulfate sodium (DSS)-induced colitis in mice. *Curr Protoc Immunol* **104**, Unit 15 25, doi:10.1002/0471142735.im1525s104 (2014).

24 Suzuki, K. *et al.* Pivotal Role of Carbohydrate Sulfotransferase 15 in Fibrosis and Mucosal Healing in Mouse Colitis. *PloS one* **11**, e0158967, doi:10.1371/journal.pone.0158967 (2016).

25 Rigottier-Gois, L. Dysbiosis in inflammatory bowel diseases: the oxygen hypothesis. *ISME J* **7**, 1256-1261, doi:10.1038/ismej.2013.80 (2013).

26 Kearns, D. B. & Losick, R. Swarming motility in undomesticated Bacillus subtilis. *Molecular microbiology* **49**, 581-590 (2003).

27 Kearns, D. B., Chu, F., Rudner, R. & Losick, R. Genes governing swarming in Bacillus subtilis and evidence for a phase variation mechanism controlling surface motility. *Molecular microbiology* **52**, 357-369, doi:10.1111/j.1365-2958.2004.03996.x (2004).

28 Sasaki, Y., Fukuda, S., Mikam, T. & Hada, R. Endoscopic quantification of mucosal surface roughness for grading severity of ulcerative colitis. *Digest Endosc* **20**, 67-72, doi:10.1111/j.1443-1661.2008.00778.x (2008).

bioRxiv preprint doi: https://doi.org/10.1101/759886; this version posted September 8, 2019. The copyright holder for this preprint (which was not certified by peer review) is the author/funder. All rights reserved. No reuse allowed without permission.

Acknowledgements

We thank Steve Almo, Cait Costello, Jeffrey Pessin, Matthew R. Redinbo and John March for valuable discussions. We aslo thank Brad Tricomi for developing the assay "Cytotoxicity of DSS on Caco-2 cell lines in the presence or absence of viable SM3 cells", Ehsan Khafipour for providing pig specimens (feces) and performing clinical scoring of histopathology, Cori Bargmann at Rockfeller University for gifting us the bacterial strains *Serratia marcescens* Db10 and *Serratia marcescens* JESM267, and Barry Bochner at Biolog Inc., California for Biochemical characterization and antimicrobial resistance profile of *Enterobacter* sp. SM1, SM2 and SM3. The studies presented here were supported in part by the Broad Medical Research Program at CCFA (Crohn's & Colitis Foundation of America; Grant# 362520) (to S.M); NIH R01 CA127231; CA 161879; 1R01ES030197-01 and Department of Defense Partnering PI (W81XWH-17-1-0479; PR160167) (S.M.), Diabetes Research Center Grant (P30 DK020541); Cancer Center Grant (P30CA013330 PI: David Goldman); 1S10OD019961-01 NIH Instrument Award (PI: John Condeelis); LTQ Orbitrap Velos Mass Spectrometer System (1S10RR029398); and NIH CTSA (1 UL1 TR001073). Peer Reviewed Cancer Research Program Career Development Award from the United States Department of Defense (CA171019, PI: Libusha Kelly). Additional invaluable assistance was obtained from Amanda Beck DVM (Histology and Comparative Pathology Core, Albert Einstein College of Medicine, Bronx, NY), Olga C. Arionadis, Thomas Ullmann and Azal Al Ani (Department of Medicine, Albert Einstein College of Medicine, Bronx, NY), Winfred Edelmann and Eleni Tosti (Department of Cell Biology, Albert Einstein College of Medicine, Bronx, NY).

Author Contributions

H.L., S.M. conceptualized the discovery. H.L., D.K., W.C., J.T., S.M. designed and executed the swarming assays. D.L. was the Principal Investigator of the Clinical Study and provided specimens. L.K. performed genome assembly and annotation. J.W., R.L., S.M. designed and executed all the 16S, metagenomic and strain-specific PCR assays. A.D. designed; A.D., W.C., S.M., S.G. characterized bacterial mutants. B.S.Y. and M.V-K. performed several swarming repeat assays and performed animal studies for reproducibility. A.D., H.L., W.C. and S.M. wrote and edited the paper. S.C. and W.C. performed statistical analyses. X.L. assisted H.L. in mouse model studies. A.B. analyzed the clinical data and revised the paper. K.S. did the histological preparations and examination. C.J. and Z.H. performed gnotobiotic mouse model studies. W.S. identified bacteria strains using MALDI-TOF.

Competing Financial Interests

Sridhar Mani, Libusha Kelly, and Hao Li filed a U.S. patent application (Application No. 62237657). Other authors declare no competing financial interests.

Materials and Correspondence

Sridhar Mani, MD
sridhar.mani@einstein.yu.edu

bioRxiv preprint doi: https://doi.org/10.1101/759886; this version posted September 8, 2019. The copyright holder for this preprint (which was not certified by peer review) is the author/funder. All rights reserved. No reuse allowed without permission.

Methods

Isolation and identification of swarming bacteria from feces. Swarming assay was performed on Luria Bertani (LB) swarming agar medium consisting of 10 g/L tryptone (Sigma), 5 g/L yeast extract (Acumedia) 10 g/L NaCl (Fisher), and 5 g/L Agar (RPI), with some critical modifications to an established method[14]. To isolate a singular dominant swarmer from a polymicrobial mix of bacteria (such as feces), we initially focused on developing an assay to isolate swarmers using known polymicrobial mixed cultures of bacteria. Single bacterial species (up to seven strains belonging to different taxa) grown in LB (OD_{600} of 1.0-1.3) were mixed in a 1:1 ratio and, 5 µL of this mix was spotted on 0.5% agar plates. Following air drying at room temperature, the plates were incubated at 37°C, 40% RH (relative humidity) for 10 hours. Bacterial swarm front was swabbed using a sterile tooth-pick from the edge of swarming colony at different locations (see arrows, Extended Data Fig. 2) and after re-streaking on separate agar plates and scaled by growth in LB, samples were identified using Matrix-Assisted Laser Desorption Ionization-Time of Flight (MALDI-TOF) mass spectroscopy. Swarmers or hyperswarmers present in the fecal or colonoscopic samples were isolated and determined using the same approach. Fecal pellets and/or colonoscopy aspirates from the clinic and/or feces of mice and pigs were collected in sterile tubes and used for swarming assays before freezing in small aliquots at -80°C. Feces from stressed intestinal model of pigs[29] were obtained on dry ice from Ehsan Khafipour at University of Manitoba, Winnipeg, Canada. Five µL aliquots of homogenized feces at 100 mg/mL concentration in phosphate buffered saline PBS, pH 7.2 or colonoscopic aspirates were spotted on swarming agar plates (optimized to 0.5% agar) and were incubated at 37°C and 40% RH, for 120 hours. Most swarming bacteria, however, were detected within the first 48-72h from incubation. Dominant swarmers from the edge of the colony were identified using MALDI-TOF.

bioRxiv preprint doi: https://doi.org/10.1101/759886; this version posted September 8, 2019. The copyright holder for this preprint (which was not certified by peer review) is the author/funder. All rights reserved. No reuse allowed without permission.

Once identified, cells from the same aliquot were plated on to 1.5% LB agar and serially passaged from a single colony to obtain a pure culture of the strain.

Bacterial swarming and time-lapse imaging. Swarming ability of a single bacterial species using a pure culture of *Enterobacter* sp. SM1 and its isogenic mutant, *Enterobacter* sp. SM3 and its transposon mutants, *Serratia marcescens* Db10 and JESM267, clinical isolate of *Serratia marcescens*, *Bacillus subtilis* 3610 and its isogenic mutant DS215 was always determined on LB swarming agar at 37°C and 40% RH prior to any experiments using these strains. *B. subtilis* 3610 and its isogenic mutant were compared on LB swarming agar containing 0.7% agar[30]. Briefly, 2 µL of an overnight culture grown in LB medium from a glycerol stock was spotted on swarming agar plate, followed by air drying at room temperature and incubating the plate overnight as stated above. Freshly made swarming agar plates, no more than 12 hours old when stored at 4°C, were used throughout the study. In order to capture real time swarming motility, a temperature and humidity controlled incubator equipped with time lapse photography was built (see accompanying publication on Nature Protocol Exchange for detailed protocol, doi:10.21203/rs.2.9946/v1). As swarming is dependent upon RH[9], we used an optimized RH of 40% that allowed image capturing without condensation on the lid of the Petri dish. Unless otherwise stated, swarming potential of isogenic strains was always compared on the same swarming agar plate to nullify the difference due to the condition of the medium, which may vary between plates. Swarming area or speed was calculated using a python based script (available online, via Nature Protocol Exchange) to identify the swarming edge using the time-lapse images. Swarming under anerobic condition (0.1 ppm) and 10% oxygen (3.3 ppm) were performed at 37°C and 40% RH in an anaerobic chamber (Coy Labs Inc.).

bioRxiv preprint doi: https://doi.org/10.1101/759886; this version posted September 8, 2019. The copyright holder for this preprint (which was not certified by peer review) is the author/funder. All rights reserved. No reuse allowed without permission.

Dextran Sulphate Sodium (DSS) induced acute colitis in conventional and gnotobiotic mice. Four to six week old female C57BL/6 mice (Jackson Laboratories, Bar Harbor, ME; # 000664) were purchased and co-housed for acclimatization at The Albert Einstein College of Medicine vivarium for 2 weeks prior to randomization by coin toss as previously described[31]. To induce acute colitis, mice were administered 3% (w/v) DSS (MW 36-50 KDa) (MP Biomedicals, LLC; Cat. no. 160110) in animal facility drinking water throughout the course of the experiment. By contrast, the control group or the normal mice always received animal facility drinking water. To determine the effect of swarming and non-swarming strains during colitis, mice were orally gavaged with 100 µL (~ 4×10^9 CFU/mL) test bacteria or LB as vehicle, daily for 9-12 days until the weight of vehicle group dropped >20%. Daily gavage of bacterial strains absolutely required use of unwashed bacterial strains grown in fresh LB (OD_{600} ~ 1.0). Mice underwent daily monitoring for body weight, clinical signs and symptoms (e.g., occult blood, diarrhea, activity), gross water consumption (measuring water marked level), and visual inspection of rectal mucosa. At the end of the experiment, mice were euthanized using isoflurane anesthesia and intestines harvested for histopathology. The histology slides were prepared using a swiss role technique of intestines embedded in paraffin as previously published[32]. Scoring of inflammatory pathology was based on a published reference with minor modifications[33]. The experimenter was not blinded to treatment allocation; however, the pathologist (KS) evaluating histologic scores was blinded to treatment allocation. All studies were approved by the Institute of Animal Studies at the Albert Einstein College of Medicine, INC (IACUC # 20160706 and preceding protocols).

Colitis was induced in five-week old germ-free (GF) wild type (WT) C57BL/6 mice under specific pathogen free (SPF) conditions[34] using 3% DSS in drinking water and treated with 100 µL (~ 4×10^9 CFU/mL) of test strain or LB as vehicle for 7 days when most mice had >10%

bioRxiv preprint doi: https://doi.org/10.1101/759886; this version posted September 8, 2019. The copyright holder for this preprint (which was not certified by peer review) is the author/funder. All rights reserved. No reuse allowed without permission.

weight drop. Mice were euthanized by CO_2 asphyxiation and histology specimens were prepared using swiss roll technique. Scoring of inflammatory pathology was based on a published reference with minor modifications[33]. All GF mouse protocols were approved by the Institutional Animal Care and Use Committee of the University of Florida (IACUC # 201308038). The experimenter (ZH, CJ) was not blinded to treatment allocation; however, the pathologist (KS) evaluating histologic scores was blinded to treatment allocation. In addition, a second pathologist (QL), randomly re-read a subset of the colitis histology slides which had a high correlation with original pathologist read (KS) (Spearman $\rho = 0.96$, 95% CI 0.92 – 0.98, $P < 0.0001$, two-tailed).

DSS-induced intestinal injury recovery model. In a study to determine the healing effect of SM3 in colitis, C57BL/6 mice were administered 3% DSS in drinking water for 7 days (when most mice had a weight loss >10% of their pre-DSS exposure weight). Subsequently, mice received animal facility drinking water without DSS and were further randomized by coin-toss to a treatment group delivered 4×10^9 CFU/mL of bacterial cells or LB by oral gavage for 5 days. Colon samples were prepared for Hematoxylin-Eosin (H&E) staining and histology and processed as described above. The precise number of mice used for each experiment are stated in the Figure legends and are visible as separate dots in the graph. In the preliminary experiments (see Fig. 2d and 4c), the computed means (± SD's) of the inflammation score for vehicle [7.28 – 9.28 (+ 1.77 – 2.4)] and wild type bacteria gavaged mice [2.59–5.66 (+ 1.31 – 3.2)] allowed for determination of the D value (~ ranging between 2-3). The exact sample size was determined under consideration of the D value, available mice per order, and ethical aspects (implementing replication studies, use of coin toss 1:1 randomization, and cage space at any given time point) as well as an assumed estimated inflation factor of ≤ 10%. For certain experiments, if insufficient

bioRxiv preprint doi: https://doi.org/10.1101/759886; this version posted September 8, 2019. The copyright holder for this preprint (which was not certified by peer review) is the author/funder. All rights reserved. No reuse allowed without permission.

number of mice were available for a reliable significance prediction, biologically independent repetition experiments were performed and data pooled for analysis (e.g., Fig. 2a-f, Fig. 4a-e).

Construction of transposon mutants. In order to generate an isogenic non-swarmer strain of SM3, we adopted an *in vivo* transposition approach using pSAM_Ec with some modifications[35]. pSAM_Ec was a gift from Matthew Mulvey (Addgene plasmid #102939; http://n2t.net/addgene:102939; RRID: Addgene_102939). In short, donor strain – EcS17/pSAM_Ec was grown from an overnight culture in pre-mating medium (M9 salts containing 40 µg/mL threonine and proline, 1 µg/mL of thiamine) with 0.2% glucose until mid-exponential phase (OD_{600} 0.5-0.6). Similarly, the recipient strain SM3 was grown in pre-mating medium containing 0.4% lactose until early exponential phase (OD_{600} 0.2-0.3). After heat shock treatment of the recipient strain at 50°C for 30 minutes the cell density of SM3 was scaled up to obtain similar number of cells as that of the donor strain. For conjugation, 750 µL of both the strains were mixed, the cells were washed twice in M9 salts and re-suspended again in the same medium. The mixture of donor and recipient was placed on a sterile 0.45 µm membrane disc (Millipore) rested on mating agar plate (1x M9-thr-pro-thi-glucose agar) and incubated upright at 37°C overnight. Next day, the cells were dislodged from the membrane in M9 medium by vortexing and plated on selective agar medium (1x M9-thr-glucose-kan agar) containing kanamycin. Individual colonies were spotted on LB swarm agar plate to screen non-swarming isogenic strain of SM3. The presence of transposon was confirmed by using transposon specific primer while the location of transposon insertion was verified by APPCR[36] followed by sequencing and mapping into the SM3 genome (Extended Data Table 2).

16S rRNA profiling to identify shift in colon microbiome. 16S rRNA meta-analyses of the fecal samples from mice were conducted at Wright Labs, LLC. Fecal samples were shipped to

bioRxiv preprint doi: https://doi.org/10.1101/759886; this version posted September 8, 2019. The copyright holder for this preprint (which was not certified by peer review) is the author/funder. All rights reserved. No reuse allowed without permission.

Wright Labs, LLC on dry ice, and underwent DNA isolation using a Qiagen DNeasy Powersoil DNA Isolation kit following the manufacturer's instructions (Qiagen, Frederick, MD). DNA was quantified and checked for its quality using the double stranded DNA high sensitivity assay on the Qubit 2.0 Fluorometer (Life Technologies, Carlsbad, CA). The 16S rRNA gene was amplified using Illumina iTag Polymerase Chain Reactions (PCR) based on the Earth Microbiome Project's 16S rRNA amplification protocol[37]. Amplified DNA was pooled, gel purified at ~ 400 bp and multiplexed with other pure libraries to form a sequencing library normalized to the final concentration of library observed within each sample. The sequencing library was sequenced using an Illumina MiSeq V2 500 cycle kit cassette with 16S rRNA library sequencing primers set for 250 base pair (bp) paired-end reads at Laragen Inc (Culver City, CA). The paired-end sequences were merged with a minimum overlap of 200 bases, trimmed at a length of 251 bp, and quality filtered at an expected error of less than 0.5% using USEARCH[38]. The reads were analyzed using the QIIME 1.9.1 software package[39,40]. Chimeric sequences were identified and assigned operational taxonomic units (OTU) using UPARSE at 97% identity[41]. The taxonomy was assigned using the Greengenes 16S rRNA gene database (13.5 release)[42]. Linear discriminant analysis (LDA) Effect Size (LEfSe) analysis was conducted to identify significantly enriched taxa within categorical groups of interest[43]. For all comparisons, a Kruskal-Wallis alpha (α) was set at 0.05 to identify significantly enriched taxa, and a pairwise Wilcoxon rank sum test was utilized to test biological consistency across all subgroups ($\alpha = 0.05$). Linear discriminant analysis (LDA) was calculated to determine effect size, and the 5 most strongly enriched taxa within each cohort were plotted. Co-occurrence network analysis was conducted on an unrarified OTU table containing bacterial abundance data from DSS + SM3

bioRxiv preprint doi: https://doi.org/10.1101/759886; this version posted September 8, 2019. The copyright holder for this preprint (which was not certified by peer review) is the author/funder. All rights reserved. No reuse allowed without permission.

treated samples and created within the Cytoscape plugin Conet[44,45]. A spearman's rho threshold of | 0.7 | was implemented prior to network plotting.

Measurement of microlevels of oxygen in mouse lumen. Oxygen concentration in the mouse lumen was assessed using a profiling oxygen microsensor (Presens IMP-PSt7-02) with a flat tip that has the ability to detect 0-1400 μM oxygen at accuracy of ± 3%. The control or DSS treated mice were first anesthetized in isoflurane for at least 3 minutes, and then the microsensor probe was inserted from the anal verge. The oxygen concentration was monitored for one minute at different locations across the colon (0.5, 1 and 2 cm from the anus) using "Presens Measurement Studio 2 (version 3.0.1.1413)". In order to avoid damage of the probe and mucosa while inserting through the anus, we used an Ethylenetetrafluoroethylene (ETFE) tube (outer diameter: 1mm; inner diameter: 0.7 mm) to house the probe. The housing was retracted to expose the probe in the designated location and cleaned before moving to the next location within the colon.

Consumption of residual oxygen on swarming plates. Swarming plates were prepared as described above and a fine hole (3 mm × 1 mm) was made on the lid of the plate to fix a syringe based oxygen microsensor probe (Presens, NTH-PSt7-02). After inoculation of the test bacterial culture, the probe was inserted into the swarming agar medium through the hole on the lid, finely adjusted using a manual micromanipulator (Presens) and then sealed using silicon oil. The side of the Petri dish was sealed using parafilm, and this whole unit was placed in the indigenously built environmental controlled incubator at 37°C. The oxygen consumption within the agar plate over time was monitored every 5 minutes for 20 hours using "Presens Measurement Studio 2". The average oxygen consumption rate in a sealed container was calculated by dividing the change in oxygen concentration with time at which the oxygen levels reached a plateau phase. Consistently, we have observed that during hyperswarming activity of SM3, the plateau phase

bioRxiv preprint doi: https://doi.org/10.1101/759886; this version posted September 8, 2019. The copyright holder for this preprint (which was not certified by peer review) is the author/funder. All rights reserved. No reuse allowed without permission.

remains stable after reaching an oxygen concentration of 0.003 ppm. This validates that the system used in this study was properly sealed from the outside environment.

Swarming on mucosal surface. We used colon tissue from mice that had received 3% DSS water or water for 10 days to develop a mucosal race experiment. Normal or DSS treated mice were euthanized, and the large intestines were cut open and cleaned to remove residual feces. After rinsing thoroughly twice in 35% (v/v) ethanol and PBS, the intestines were sectioned into small segments of around 1.5-2.5 cm each. A hybrid plate with sterile swimming agar (3 g/L) and hard agar (15 g/L) was prepared, where one half of the plate had 1.5% agar and the other half was filled with 0.3% agar containing LB. To make such hybrid agar plate, 1.5% agar was poured first and once solidified half of the gel was removed using a sterilized spatula to fill the rest of the Petri dish with the heated mix that forms the swimming agar. The tissue pieces were placed on 1.5% agar in a way so that the other end of the tissue exactly overlapped with the border between 1.5% agar and the swimming agar. Overnight bacterial cultures were serially diluted 10^{12} times to reach cell concentration of 10^{6} CFU/mL, 2 μL of which was inoculated on a 2 mm × 2 mm sterilized filter membrane (MF-Millipore, 0.45 μm). This allowed absorption of liquid broth while adsorbing the bacterial cells on the membrane surface. The membrane was then used as a source of inoculum on the mucosal surface. The motility of a non-swarmer and a swarmer was always compared using a piece of tissue that belonged to the same region of the colonin mice. The plates were dried in the laminar hood for 20-30 minutes before incubating at 37ºCand 40% RH overnight. Drying of plates allowed removal of excess moisture from the topmost layer of the tissue. Time-lapse photos were captured to evaluate the time at which bacterial test strain reached the other end of the intestinal tissue indicated by the swimming of bacteria on 0.3% LB agar. Distance travelled by the bacterial strain was measured in ImageJ

bioRxiv preprint doi: https://doi.org/10.1101/759886; this version posted September 8, 2019. The copyright holder for this preprint (which was not certified by peer review) is the author/funder. All rights reserved. No reuse allowed without permission.

according to the pixel/length ratio. The motility rates were calculated as Distance travelled / Time duration in which the test strain reached the swim agar.

Statistical analysis. *P* values of data were obtained by parametric or non-parametric methods, as indicated in the figure legends, with 95% confidence interval (CI). Normality (Gaussian distribution) was not assumed and for each dataset this was either tested for or transformed (e.g., log normality) to discern whether the data fit a Gaussian distribution. Through visual inspection, sample size assessment, and tests for normality, a determination was made to use a parametric or non-parametric statistical test, as indicated. All statistical tests, except where otherwise indicated, were performed with Graph Pad Prism v.8.2.0; * $P < 0.05$, ** $P < 0.01$, *** $P < 0.001$; ns, not significant. All plots are shown as mean and 95% CI except where otherwise indicated.

bioRxiv preprint doi: https://doi.org/10.1101/759886; this version posted September 8, 2019. The copyright holder for this preprint (which was not certified by peer review) is the author/funder. All rights reserved. No reuse allowed without permission.

Methods References

29 Munyaka, P. M., Sepehri, S., Ghia, J. E. & Khafipour, E. Carrageenan Gum and Adherent Invasive Escherichia coli in a Piglet Model of Inflammatory Bowel Disease: Impact on Intestinal Mucosa-associated Microbiota. *Frontiers in microbiology* **7**, 462, doi:10.3389/fmicb.2016.00462 (2016).

30 Kearns, D. B. & Losick, R. Cell population heterogeneity during growth of Bacillus subtilis. *Genes Dev* **19**, 3083-3094, doi:10.1101/gad.1373905 (2005).

31 Venkatesh, M. *et al.* Symbiotic bacterial metabolites regulate gastrointestinal barrier function via the xenobiotic sensor PXR and Toll-like receptor 4. *Immunity* **41**, 296-310, doi:10.1016/j.immuni.2014.06.014 (2014).

32 Whittem, C. G., Williams, A. D. & Williams, C. S. Murine Colitis modeling using Dextran Sulfate Sodium (DSS). *Journal of visualized experiments : JoVE*, doi:10.3791/1652 (2010).

33 Erben, U. *et al.* A guide to histomorphological evaluation of intestinal inflammation in mouse models. *Int J Clin Exp Pathol* **7**, 4557-4576 (2014).

34 McCafferty, J. *et al.* Stochastic changes over time and not founder effects drive cage effects in microbial community assembly in a mouse model. *ISME J* **7**, 2116-2125, doi:10.1038/ismej.2013.106 (2013).

35 Wiles, T. J. *et al.* Combining quantitative genetic footprinting and trait enrichment analysis to identify fitness determinants of a bacterial pathogen. *PLoS Genet* **9**, e1003716, doi:10.1371/journal.pgen.1003716 (2013).

36 Saavedra, J. T., Schwartzman, J. A. & Gilmore, M. S. Mapping Transposon Insertions in Bacterial Genomes by Arbitrarily Primed PCR. *Curr Protoc Mol Biol* **118**, 15 15 11-15 15 15, doi:10.1002/cpmb.38 (2017).

37 Walters, W. *et al.* Improved Bacterial 16S rRNA Gene (V4 and V4-5) and Fungal Internal Transcribed Spacer Marker Gene Primers for Microbial Community Surveys. *mSystems* **1**, doi:10.1128/mSystems.00009-15 (2015).

38 Edgar, R. C. Search and clustering orders of magnitude faster than BLAST. *Bioinformatics* **26**, 2460-2461, doi:10.1093/bioinformatics/btq461 (2010).

39 Caporaso, J. G. *et al.* QIIME allows analysis of high-throughput community sequencing data. *Nat Methods* **7**, 335-336, doi:10.1038/nmeth.f.303 (2010).

40 Caporaso, J. G. *et al.* Global patterns of 16S rRNA diversity at a depth of millions of sequences per sample. *Proceedings of the National Academy of Sciences of the United States of America* **108 Suppl 1**, 4516-4522, doi:10.1073/pnas.1000080107 (2011).

41 Edgar, R. C. UPARSE: highly accurate OTU sequences from microbial amplicon reads. *Nat Methods* **10**, 996-998, doi:10.1038/nmeth.2604 (2013).

42 DeSantis, T. Z. *et al.* Greengenes, a chimera-checked 16S rRNA gene database and workbench compatible with ARB. *Appl Environ Microbiol* **72**, 5069-5072, doi:10.1128/AEM.03006-05 (2006).

bioRxiv preprint doi: https://doi.org/10.1101/759886; this version posted September 8, 2019. The copyright holder for this preprint (which was not certified by peer review) is the author/funder. All rights reserved. No reuse allowed without permission.

43 Segata, N. *et al.* Metagenomic biomarker discovery and explanation. *Genome Biol* **12**, R60, doi:10.1186/gb-2011-12-6-r60 (2011).

44 Shannon, P. *et al.* Cytoscape: a software environment for integrated models of biomolecular interaction networks. *Genome Res* **13**, 2498-2504, doi:10.1101/gr.1239303 (2003).

45 Faust, K. & Raes, J. CoNet app: inference of biological association networks using Cytoscape. *F1000Research* **5**, 1519, doi:10.12688/f1000research.9050.2 (2016).

46 Lee, K., Tosti, E. &Edelmann, W. Mouse models of DNA mismatch repair in cancer research. *DNA Repair*, **38**, 140-146, doi:10.1016/j.dnarep.2015.11.015 (2016).

bioRxiv preprint doi: https://doi.org/10.1101/759886; this version posted September 8, 2019. The copyright holder for this preprint (which was not certified by peer review) is the author/funder. All rights reserved. No reuse allowed without permission.

Extended Data Figure 1

a

		Disease*	
		+	-
Age	Mean (± SD)	51 ± 14	50 ± 11
	Median (Range)	52 (21-81)	51 (24-70)
Gender	Females	27	8
	Males	17	9

* Defined as individuals with clinically established *active* inflammatory bowel disease (Crohn's disease n = 14, or Ulcerative colitis n = 5), intestinal dysplasia (n =1), intestinal polyps (n = 23), intestinal reactive hyperplasia and inflammatory changes not otherwise specified (n = 1). All other diagnoses were considered "negative" for disease.

b

		Disease*	
		+	-
Swarming test †	+	25	3
	-	20	22

* One patient consented for the study specimen but did not undergo colonoscopy; One patient had a poor colonoscopy preparation and aspirate sample was not obtained; 9 fecal samples obtained from OpenBiome (Boston, MA), one of which was contaminated inadvertently with a laboratory swarming strain and was excluded from analysis.
† "Postive" defined as swarming score ≥ 1; "negative" defined as swarming score = 0.

c

Statistic*	Value	95% CI†
Sensitivity	55.56%	40.00% to 70.36%
Specificity	88.00%	68.78% to 97.45%
Positive Likelihood Ratio	4.63	1.55 to 13.81
Negative Likelihood Ratio	0.51	0.35 to 0.72
Disease Prevalence	64.29%	51.93% to 75.39%
Positive Predictive Value	89.29%	73.63% to 96.13%
Negative Predictive Value	52.38%	54.88% to 77.91%

* Computed with: https://www.medcalc.org/calc/diagnostic_test.php
† CI, confidence interval

d

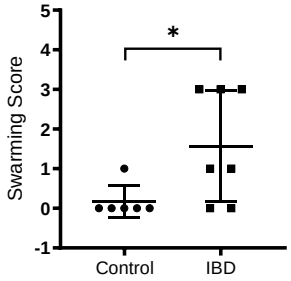

e

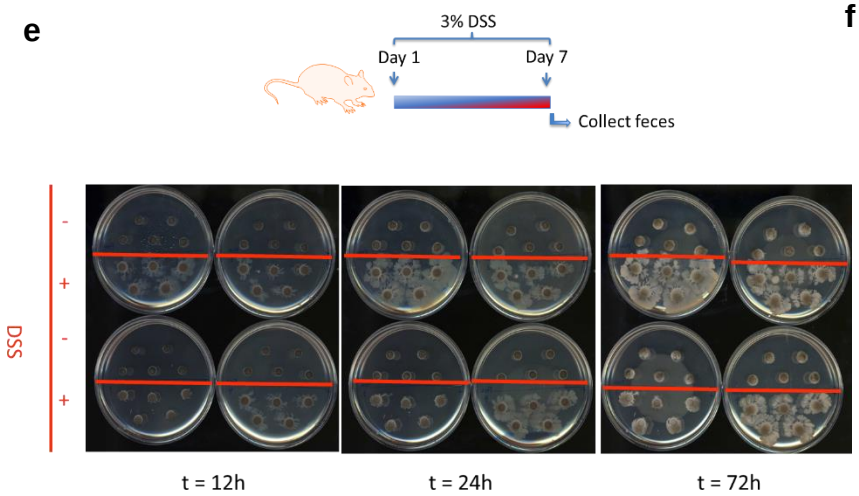

f

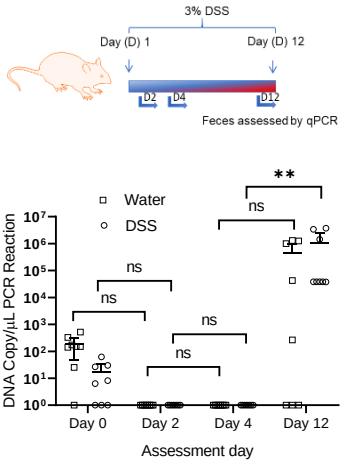

Extended Figure 1 | Effect of intestinal inflammation on bacterial swarming. a-c, Human colonoscopy aspirates (n = 45 intestinal disease; n = 25 non-disease) were spotted on 0.5% agar plates and the swarming assay performed. **a,** Colonoscopic washes were obtained from individuals with active intestinal disease and matched controls. Swarming assays performed using aspirates were binned by disease as defined both clinically and by intestinal histopathology, where available. **b,** Clinical demographics are described for the disease and non-disease population**. c,** Swarming assays test statistics. **d,** Swarming assays (72h) of fecal samples collected from pigs with and without IBD. Swarming scores - 0: no swarming, 1: swarming within 72h, 2: swarming within 48h, 3: swarming within 24h or less (Control: n = 6; IBD: n = 7). **e,** C57BL/6 mice (8-week old) were exposed to water or DSS water for 7 days (n = 4 per group). Fecal samples of control group (above red line) and DSS group (below red line) were collected for swarming assay. Swarming plates were scanned at 12, 24 and 48 hours**. f,** In a separate experiment, C57BL/6 mice (8-week old) were exposed with water or DSS water for 12 days (n = 8 per group). Fecal samples were collected for DNA extraction and SM1/SM3-specific PCR analysis was performed, and DNA copy number ascertained. Unless otherwise noted, data represented as mean and 95% CI, and significance tested using two-way ANOVA followed by Tukey's post hoc test. **d,** significance tested using Welch's t-test. IBD, Inflammatory Bowel Disease.

bioRxiv preprint doi: https://doi.org/10.1101/759886; this version posted September 8, 2019. The copyright holder for this preprint (which was not certified by peer review) is the author/funder. All rights reserved. No reuse allowed without permission.

Extended Data Figure 2

a

Top

Middle

Bottom

b

Sample Number	MALDI Identification	MALDI Identification Score (Mean) *
A-1	*Klebsiella pneumoniae* *Escherichia coli*	2.26 2.06
A-2	*Klebsiella pneumoniae* *Escherichia coli*	2.24 2.33
A-3	*Klebsiella pneumoniae* *Escherichia coli* *Acinetobacter sp.*	2.20 2.33 1.82
A-4	*Klebsiella pneumoniae* *Acinetobacter sp.*	2.12 1.76
A-5	*Klebsiella pneumoniae*	2.12
A-6	*Klebsiella pneumoniae* *Escherichia coli*	2.24 2.14
B-1	*Bacillus sp.*	1.81
B-2	*Bacillus sp.*	1.83
B-3	*Bacillus sp.*	1.79
B-4	*Bacillus sp.*	1.80
B-5	*Bacillus sp.*	1.80
B-6	*Bacillus sp.*	1.84
C-1	*Enterobacter asburiae*†	2.24
C-2	*Enterobacter asburiae*	2.28
C-3	*Enterobacter asburiae*	2.31
C-4	*Enterobacter asburiae*	2.25
C-5	*Enterobacter asburiae*	2.27
C-6	*Enterobacter asburiae*	2.21

* MALDI identification scores ≥ 2.0 indicate reliable species level identification. Identification scores between 1.7-1.99 indicate a reliable identification to the genus level only.

† *Enterobacter asburiae* is a member of *Enterobacter cloacae* complex. The species level identification *of E. cloacae* complex members by MALDI was confirmed using 16S sequencing.

Extended Data Figure 2 | Identification of dominant swarming bacteria within a polymicrobial culture. a, 1:1 ratio mix of bacteria were used for swarming assay on 0.5% LB agar for 10 hours. *Top*: five non-swarming bacteria were mixed and applied on 0.5% agar. Six random picks as shown in arrows were placed on the edge of colony (1. *Klebsiella pneumoniae* 2. *Escherichia coli* 3. *Acinetobacter* sp. 4. *Bordetella hinzii* 5. *Staphylococcus xylosus*) and 1.5% LB agar streaks performed - single viable colonies were subjected to MALDI-TOF identification. *Middle*: five non-swarming bacteria as above plus two known hyperswarming bacteria SM3 (*Enterobacter asburiae*) and *Bacillus* sp. were mixed, and experiment repeated as per *Top* panel. Six random picks as shown in arrows were placed on the edge of the complex. *Bottom*: five non-swarming bacteria as above plus one known hyperswarming bacteria SM3 (*Enterobacter asburiae*). Six random picks as shown in arrows were placed on the edge of complex**. b,** Table showing results of MALDI-TOF identification of bacterial colonies isolated from swarming edge. A1-A6 are picks from **a** *Top*. B1-B6 from **a** *Middle*, and C1-C6 from **a** *Bottom*. "A" represents mix of bacterial species *Klebsiella pneumoniae*, *Escherichia coli*, *Acinetobacter* sp., and *Bordetella hiuzii*, *Staphylococcus xylosus*; "B" represents mix of "A", *Bacillus pumilus*, and SM3; "C" represents mix of "A" and SM3.

bioRxiv preprint doi: https://doi.org/10.1101/759886; this version posted September 8, 2019. The copyright holder for this preprint (which was not certified by peer review) is the author/funder. All rights reserved. No reuse allowed without permission.

Extended Data Figure 3

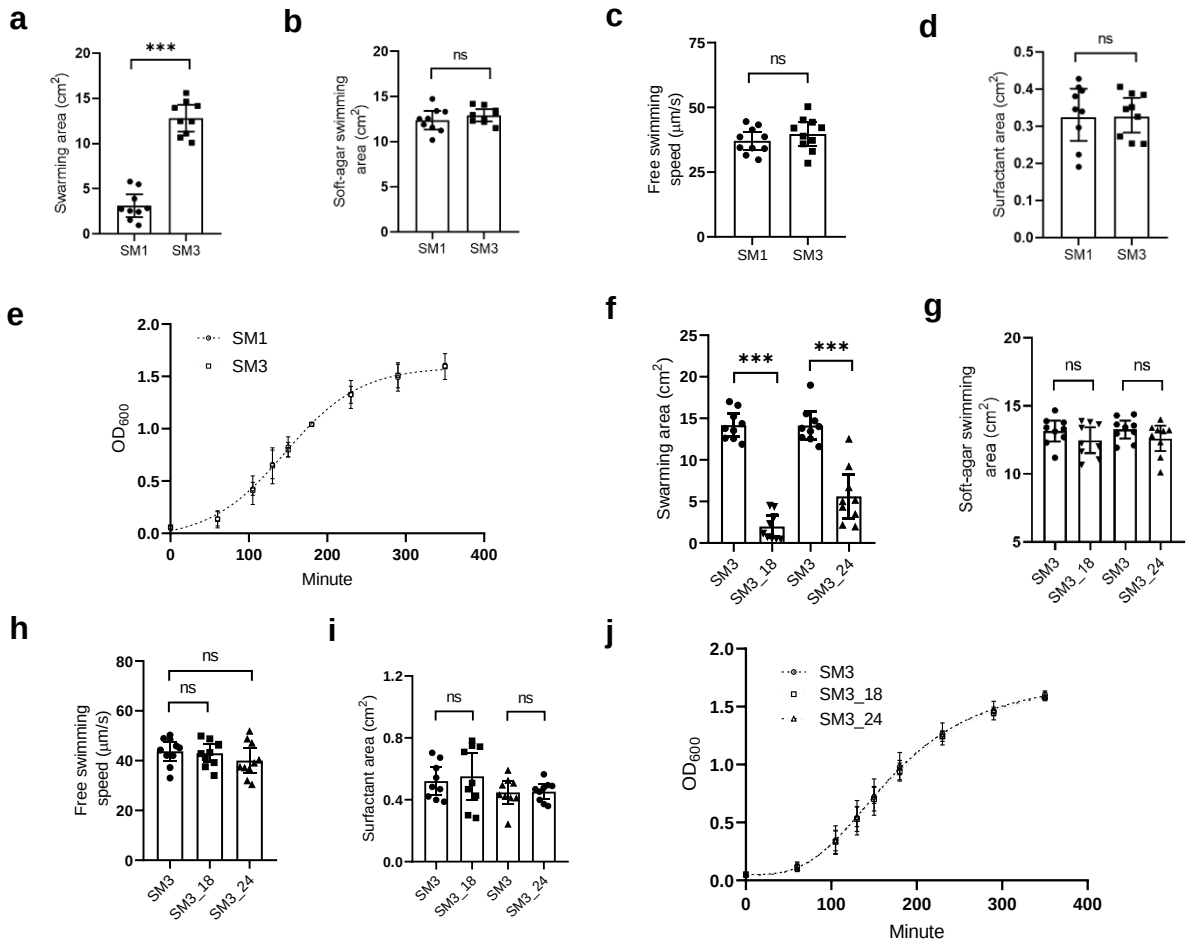

Extended Data Figure 3 | Characterization of motility, growth, and surfactant production by *Enterobacter* sp. SM1, SM3 and its mutant strains. a-e, SM3 and SM1, swarming motility (**a**), soft-agar swimming motility (**b**), free swimming motility (**c**), surfactant production (**d**) and growth rate (**e**) (n = 3, each in triplicate except for **e**, n = 3, each in singlet). **f-j,** SM3 and mutants (SM3_18 and SM3_24), swarming motility (**f**), soft-agar swimming motility (**g**), free swimming motility (**h**), surfactant production (**i**), and growth rate (**j**) (n = 3, each in triplicate except for **j**, n = 3, each in singlet). Unless otherwise noted, data are presented as mean and 95% CI, and significance tested using a two-tailed Student's t-test. **h,** significance tested using one-way ANOVA followed by Tukey's post hoc test.

bioRxiv preprint doi: https://doi.org/10.1101/759886; this version posted September 8, 2019. The copyright holder for this preprint (which was not certified by peer review) is the author/funder. All rights reserved. No reuse allowed without permission.

Extended Data figure 4

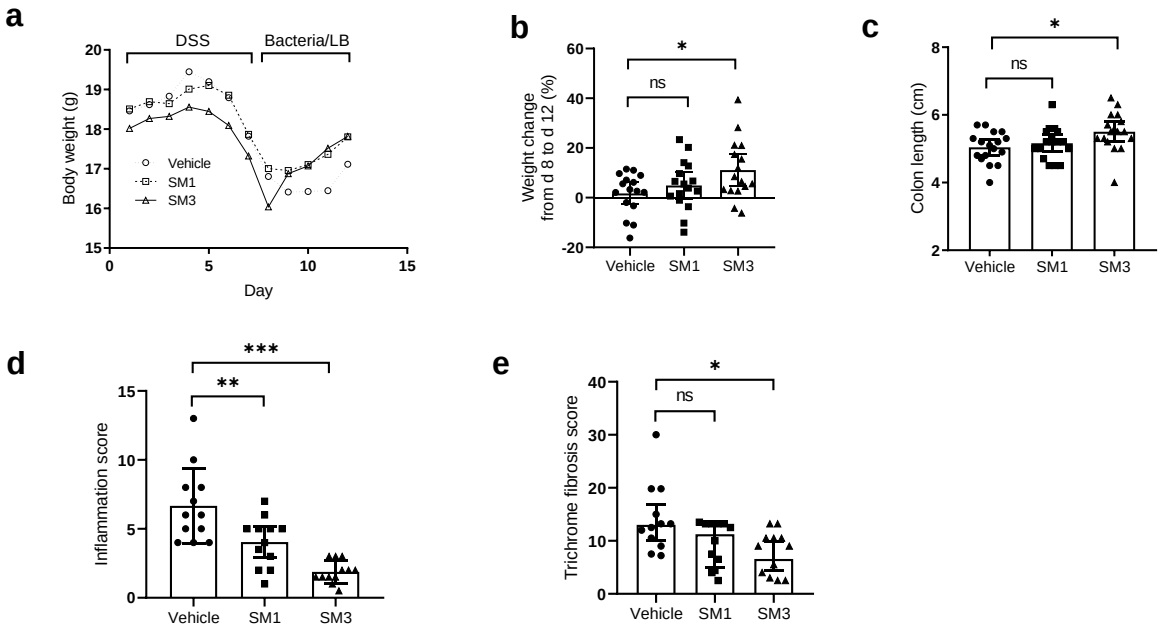

Extended Data Figure 4 | Effect of *Enterobacter* sp. SM1 or SM3 strain on DSS induced colitis in C57BL/6 mice during recovery phase. 8-week old mice were exposed to DSS water for 7 days. On day 8, DSS water was replaced with drinking water and mice were administered vehicle (LB), SM3 or SM1 for 5 days**. a-e,** indicates day by day weight change (**a**), day 8 to day 12 weight change (**b**), colon length (**c**), inflammation score (**d**), and trichrome fibrosis score **(e)** (n = 16 per treatment group except for **d** and **e**, four colon specimens per group were used for other experiments). Unless otherwise noted, data represented as mean and 95% CI, and significance tested using one-way ANOVA followed by Tukey's post hoc test. **e,** data represented as median and interquartile range, and significance tested using Kruskal-Wallis followed by Dunn's multiple comparisons test.

bioRxiv preprint doi: https://doi.org/10.1101/759886; this version posted September 8, 2019. The copyright holder for this preprint (which was not certified by peer review) is the author/funder. All rights reserved. No reuse allowed without permission.

Extended Data Figure 5

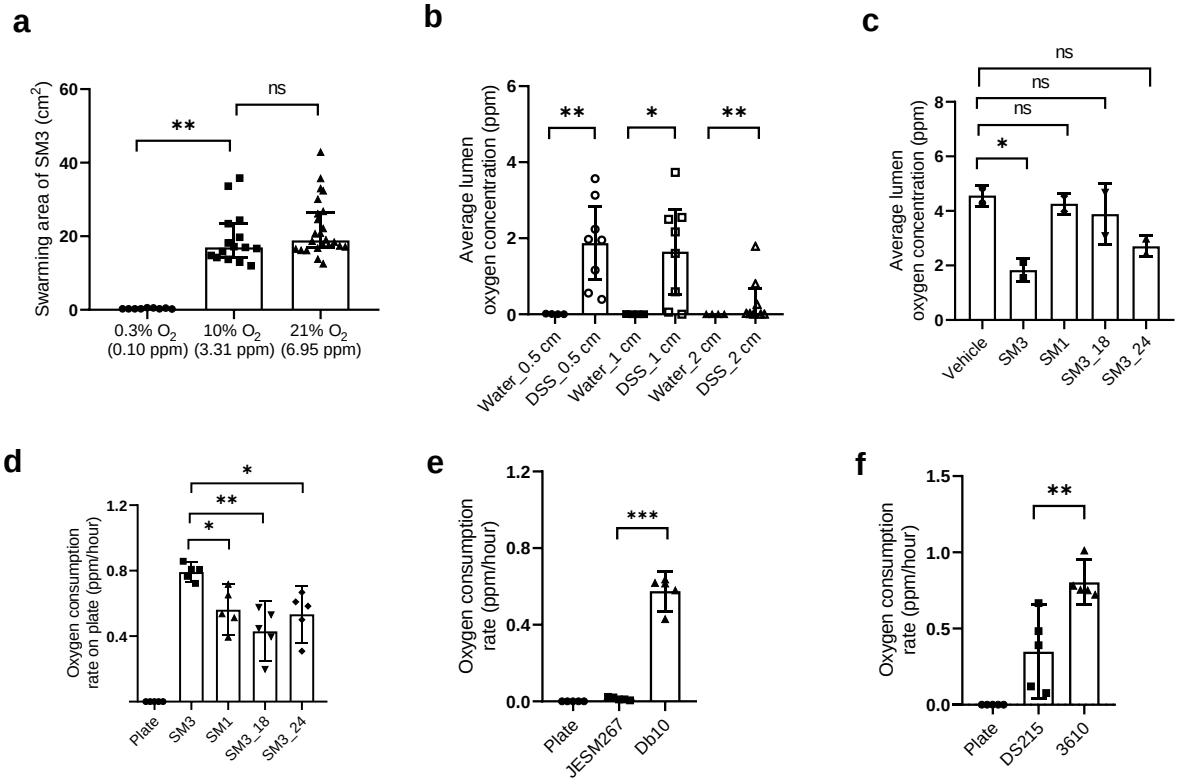

Extended Data Figure 5 | Oxygen measurements *in vivo* and *in vitro* using a microsensor probe. a, The swarming area of SM3 on LB agar plate in 8 hours under different concentration of oxygen (0.3%: n = 3, each in triplicate; 10%: n = 5, each in triplicate; 21%: n = 6, each in quadruplicate). **b,** C57BL/6 mice were exposed to water or DSS water for 10 days. Average lumen oxygen concentration (0.5, 1, and 2 cm from the anus) was measured (normal, n = 4; DSS, n = 8). **c,** In a separate experiment, C57BL/6 mice were exposed to DSS water and treated with SM1, SM3, or its mutants (SM3_18 or SM3_24) for 10 days. Average lumen oxygen concentration was measured (n = 2 per treatment group). **d-f,** Oxygen consumption rate was measured for different strains: SM1, SM3, and its mutant strains (**d**); Db10 and JESM267 (**e**); 3610 and DS215 (**f**) on LB agar plate (n = 5, each in singlet). Plate indicates oxygen consumption rate in LB agar with no bacteria. Unless otherwise noted, data are presented as mean and 95% CI, and significance tested using one-way ANOVA followed by Tukey's post hoc test. **a,** data are presented as median and interquartile range, and significance tested using Kruskal-Wallis test. **b,** for 0.5 cm and 1 cm groups, significance tested using a two-tailed Student's t-test; for 2 cm groups, data are presented as median and interquartile range, and significance tested using Mann Whitney test.

bioRxiv preprint doi: https://doi.org/10.1101/759886; this version posted September 8, 2019. The copyright holder for this preprint (which was not certified by peer review) is the author/funder. All rights reserved. No reuse allowed without permission.

Extended Data Figure 6

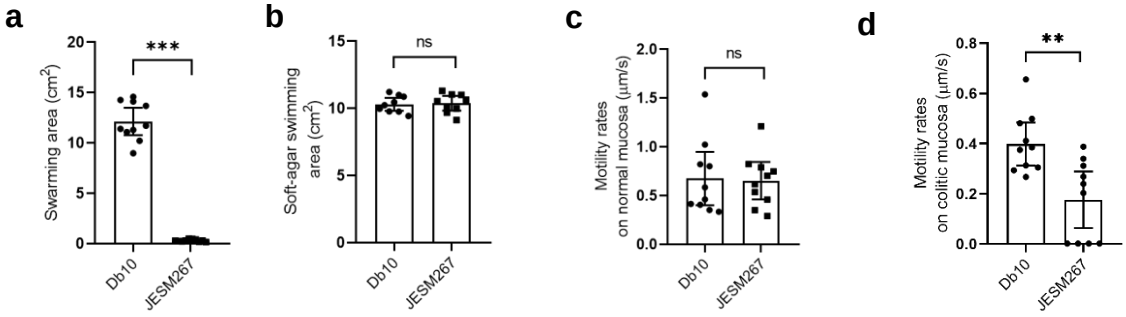

Extended Data Figure 6 | Motility rates of *S. marcescens* in different media. a-b, *S. marcescens* Db10 and *S. marcescens* JESM267, swarming motility (**a**), soft-agar swimming motility (**b**) (n = 3, each in triplicate). **c-d,** *S. marcescens* Db10 and *S. marcescens* JESM267, motility rates on normal (**c**) and colitic (**d**) mucosal surface of C57BL/6 mouse (n = 4, at least in duplicate). Unless otherwise noted, data are represented as mean and 95% CI, and significance tested using a two-tailed Student's t-test.

bioRxiv preprint doi: https://doi.org/10.1101/759886; this version posted September 8, 2019. The copyright holder for this preprint (which was not certified by peer review) is the author/funder. All rights reserved. No reuse allowed without permission.

Extended Data Figure 7

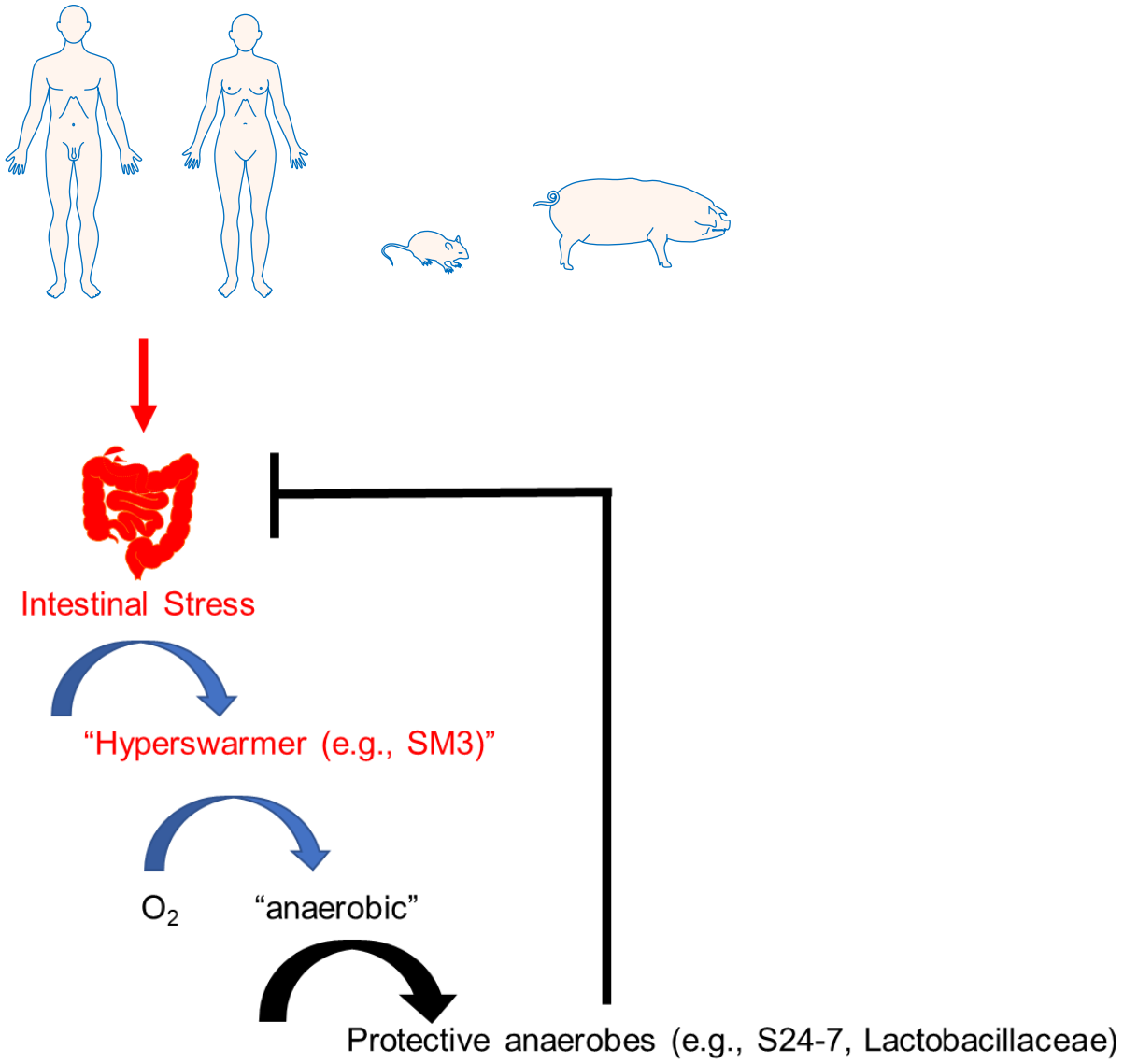

Extended Data Figure 7 | Schematic of proposed mechanism of cause and consequence of bacterial swarming during intestinal stress. Acute intestinal stress (e.g., colitis), as opposed to a homeostatic colonic lumen, induces growth of bacteria with hyperswarming properties. If the abundance of swarming bacteria has reached sufficient levels passing some threshold CFU, local luminal oxygen levels in the intestine rapidly decline, creating a favorable environment for anaerobes. The bloom of protective anaerobes such as belonging to family Bacteriodales S24-7 and Lactobacillaceae in turn correlates with the accelerated resolution of inflammation and healing in colitic mice. Thus, bacterial hyperswarming is a protective response to intestinal stress and one that is garnered during the evolution of colitis. CFU, Colony Forming Units.

bioRxiv preprint doi: https://doi.org/10.1101/759886; this version posted September 8, 2019. The copyright holder for this preprint (which was not certified by peer review) is the author/funder. All rights reserved. No reuse allowed without permission.

Extended Data Table 1 | Isolation of Bacterial Strains on the Swarming Assay from Feces *

Sample	Swarming	Strain Isolated
Human IBD	+	*Escherichia coli* #
Human IBD	+	*Escherichia coli* #
Human anal fistula	+	*Escherichia coli*
Human IBD	+ †	*Klebsiella pneumoniae*
Healthy Human	- ‡	*Klebsiella pneumoniae*
Human IBD	+	*Citrobacter koseri*
Human IBD	- §	*Morganella morganii*
Human adenomatous polyp	+	*Serratia marcescens*
Mouse colitis	+ ‖	*Proteus mirabilis*
Mouse colitis	+ ¶	*Proteus mirabilis*
Mouse (DSS colitis)	+	*Enterobacter sp.* #
Mouse (TNBS colitis)	+	*Enterobacter sp.* #

* Human or mouse feces was subject to the swarming assay and any swarm colony detected within 24 h was swabbed for strain identification. In addition, delayed swarmers were classified as negative but their swarm edge also yielded single species:
† Feces from patient with clinically controlled Crohn's disease with moderate surfactant edge detected at 74 h
‡ Classified as non-swarmer; however, a very minimal surfactant edge present at 24h and no progression thereafter
§ Feces from patient with clinically controlled Crohn's disease with surfactant edge detected at 48h
‖, ¶ Mouse model: Msh2/-loxPTgfbr2 loxp Villin-cre[46]
Also confirmed using Illumina Sequencing (PacBio)

bioRxiv preprint doi: https://doi.org/10.1101/759886; this version posted September 8, 2019. The copyright holder for this preprint (which was not certified by peer review) is the author/funder. All rights reserved. No reuse allowed without permission.

Extended Data Table 2 | Primers used in this study

Primers	Sequence (5' → 3')	Description
MotA_Up_F	AGCAGAATATTCACGCTTCCA	Forward primer used to amplify *mot*A upstream flanking region from SM1 genomic DNA
MotA_Up_R (BamHI)	TAATGGATCCGTAACCTAATAAGATAAGCACGACATCA *	Reverse primer used to amplify *mot*A upstream flanking region from SM1 genomic DNA
MotA_Dn_F(EcoRI)	TAATGAATTCCGATCGCGGTTGAGTTTG	Forward primer used to amplify *mot*A downstream flanking region from SM1 genomic DNA
MotA_Dn_R	CGGTTCTGGCTGTCGATAAT	Reverse primer used to amplify *mot*A downstream flanking region from SM1 genomic DNA
Kan_F(BamHI)	TAATGGATCCATGGCTAAAATGAGAATATCACC	Forward primer used to amplify Kanamycin cassette from pCAM48
Kan_R(EcoRI)	TAATGAATTCCTAAAACAATTCATCCAGTAAAATAT	Reverse primer used to amplify Kanamycin cassette from pCAM48
MotA_Up_seq_ver	AGCGAGAAAAGCATTGTTCA	Sequencing primer to verify *mot*A deletion at the 5'end in SM1
MotA_Dn_seq_ver	ATCATCAAGCCCACCTACCA	Sequencing primer to verify *mot*A deletion at the 3'end in SM1
Just_F1	GAAGAACCGCAGTATCCCGA	Forward primer for SM1 and SM3 strain specific PCR verification
Just_R1	AGTGTGCTGCGAACGTAAGG	Reverse primer for SM1 and SM3 strain specific PCR verification
pSAM_Tn_det_F	CTGAATGAACTGCAGGACGA	Forward primer to verify transposon insertion in SM3 transposon mutants
pSAM_Tn_det_R	CTGGCAGTTCCCTACTCTCG	Reverse primer to verify transposon insertion in SM3 transposon mutants
pSAM_Tn_ver_R	GCTTGCTGTCCATAAAACC	Transposon specific primer to identify its location in SM3 mutant during APPCR (cycle 1) †
pSAM_Tn_ver_F	GCTCTCCTGAGTAGGACAAA	Transposon specific primer to identify its location in SM3 mutant during APPCR (cycle 1)
Ran3_APPCR	**GTTCTACACGAGTCACTGCAG**GGTGACGCAG ‡	Random primer to identify transposon location in SM3 mutant during APPCR (cycle 1)
Ran5_APPCR	**GTTCTACACGAGTCACTGC**AGGTCTACACGG ‡	Random primer to identify transposon location in SM3 mutant during APPCR (cycle 1)
Fix_APPCR	GTTCTACACGAGTCACTGC	Primer specific to amplicon generated in APPCR (cycle 1)
pSAM_verF_APPCR2_b	CATAAACTGCCAGGCATCAA	Primer specific to amplicon generated in APPCR (cycle 1) and annealing within the transposon
SM3_18_for	GTGATGGCAATCGCGAATATCG	Forward primer to confirm transposon insertion location in the mutant SM3_18
SM3_18_rev	GTTCACAGTTCCACCTCGCTGAAG	Reverse primer to confirm transposon insertion location in the mutant SM3_18
SM3_24_for1	ATCGATACCTTATGAAAAATGTTCTG	Forward primer to confirm transposon insertion location in the mutant SM3_24
SM3_24_rev1	ATTGTCGAATTATCCATGTTGTG	Reverse primer to confirm transposon insertion location in the mutant SM3_24
Sa.en_FliL_F_FRTKan	CACGGGATAATCAGCCAATAAGCAGTACCGAAACAGGAA GCCCGTATCAGATGGTGTAGGCTGGAGCTGCTTC	Forward primer for *fliL* deletion in *Salmonella enterica*
Sa.en_FliL_R_FRTKan	CAGCCTGAGAAAGAATACTATCGCCCATATCGTTACCGC AGAATAAAAGCATGGGAATTAGCCATGGTCC	Reverse primer for *fliL* deletion in *Salmonella enterica*
Sa.en_FliL_det_F	ACGCCAGAGGTAGCATGATT	Sequencing primer to verify *fliL* deletion at the 5'end in *Salmonella enterica*
Sa.en_FliL_det_R	CTTGCGATACCGGGAGTG	Sequencing primer to verify *fliL* deletion at the 3'end in *Salmonella enterica*

* Underlined sequences represent restriction digestion site.
† APPCR, Arbitrary-Primed Polymerase Chain Reaction.
‡ Sequences in bold in the primers Ran3_APPCR and Ran5_APPCR represent sequence similarity to the primer Fix_APPCR.